

## Research Article

# About Some Fundamental Aspects of the Growth Mechanism Vapor-Liquid-Solid Nanowires

Valery A. Nebol'sin  and Nada Swaikat 

Voronezh State Technical University, Department of Radio Engineering and Electronics, Voronezh 394006, Russia

Correspondence should be addressed to Nada Swaikat; nada.s84@mail.ru

Received 20 September 2022; Revised 8 February 2023; Accepted 13 March 2023; Published 31 March 2023

Academic Editor: Marco Rossi

Copyright © 2023 Valery A. Nebol'sin and Nada Swaikat. This is an open access article distributed under the Creative Commons Attribution License, which permits unrestricted use, distribution, and reproduction in any medium, provided the original work is properly cited.

This study provides the formation of semiconductor nanowires (NWs) with a singular facet and a curved end surface by the vapor-liquid-solid (VLS) process that is analyzed and explained in details. Given the evidence, it is confirmed that the wettability of a liquid catalyst droplet on a crystal surface and the contact angle between the droplet and crystal play an essential role in the VLS process of NWs development. It is shown that for the VLS mechanism, the formation of NWs depends on the reduction in activation barrier to crystallization caused by the release of surplus-free energy by a spheroidizing drop in the region of the triple junction during the process of lowering surface area. This decreases the necessary supersaturation for the development of NW vertex facets at a fixed growth rate. The source of the extra free energy that drives the catalyst droplet movement during the steady-state development of NWs is the droplet's outer surface. During the formation of NWs, those angles of inclination of the lateral surface NWs and droplet contact are obtained at which the solid/vapor, solid/liquid, and liquid/vapor interfaces experience the smallest increase in free energy. The wetting hysteresis is demonstrated to occur at the vertex of NWs, and the contact angle of a catalyst droplet may be regarded as an independent and fully-fledged thermodynamic parameter of the system's state.

## 1. Introduction

In 2024, it will be sixty years since Wagner and Ellis discovered the nanowire growth technique [1]. It has been the subject of several studies [2–10]. In the past, the development and characteristics of crystals composed of almost two hundred elements and compounds have been investigated. Nanowires (NWs) of semiconductor materials are promising candidates for micro- and high-speed sensors, high-performance photodetectors, thermoelectric elements, field transistors, memory cells, and other nanoelectromechanical devices [9–15]. In recent years, there has been a real boom in research aimed at developing methods for the controlled production and determination of the physical characteristics of nanowires (NWs) of semiconductor materials. VLS-growth enables the bulk fabrication of structurally flawless NWs (including heterostructure ones) with precise control over their size, crystallographic orientation, and synthesis temperature (less than 400°C) at little expense. Nevertheless,

despite notable accomplishments in this regard, a unified and comprehensive knowledge of the underlying underpinnings of the VLS development process of NWs is not yet known.

The tendency of a system to lose free energy is the driving force behind every phase shift, including VLS crystallization. The free energy per unit volume of the new phase must be smaller than the free energy per unit volume of the old phase for a simple phase change to occur. However, this is a condition that is required but not sufficient. The production of particles in a new phase necessitates the development of new surfaces with greater energy, which complicates the transition. Unfortunately, the evidence on the underlying underpinnings of VLS development in NWs is fragmented, insufficient, and sometimes contradictory.

For instance, it has been shown that the free interfacial energy of the liquid/vapor, crystal/vapor, and crystal/liquid interfaces plays a crucial role in the formation of NWs (Givargizov [3]). It (energy) determines the wetting, and

consequently, specifies the shape of a drop of metal (M)-catalyst at the vertex of NWs, characterized by the contact angle, i.e., the angle between the tangent drawn to the surface of the liquid droplet and the end facet NWs, with the vertex located at the point of contact of the three phases on the droplet wetting perimeter. In turn, the contact angle pre-determines the ratio between the transverse dimensions of the NWs and the catalyst droplet, and therefore, the form of the developing crystal (Nebol'sin et al., [4]). The contact angle affects the shape of the NWs at the crystallization front. If the contact angle is minimal, then, the crystallization front under the drop is flat (Harmand et al. [10]), and if the contact angle is considerable, then, the crystallization front bends and becomes convex [11, 15–18]. Quite recently, while growing NWs under a high-resolution transmission electron microscope (TEM), it was discovered that nanowires exhibit wetted truncated facets along the crystallization front (TFL) [15, 19, 20]. In addition, the wetting and contact angle influence the circumstances that determine the crystalline phase ZB/WZ of IIIIBV nanowires (Glas et al., [7]). Under typical circumstances, the wetting angle of a drop sitting on the horizontal surface of the substrate is smaller than that of the formed nanowire; hence, the NWs narrow from the base, creating a so-called pedestal [9, 21, 22]. Nevertheless, there is evidence that NWs may emerge from droplets already containing the crystalline component without producing a cone-shaped pedestal [23, 24].

At very tiny contact angles, the catalyst droplets do not form NWs but rather pyramids or pointed hills [3]. At nonwetting and extremely large angles, there is insufficient contact between the drop and the substrate, leading to instability. During the self-catalyzed growth of NWs of complex semiconductors (for example, GaAs with the participation of a Ga-catalyst), the components of the compound typically wet the side walls of the crystal well, and to increase the contact angle, it is necessary to increase the droplet's supersaturation, which increases the risk of instabilities [3, 5, 15, 25].

Consequently, the wettability of the crystal surface by a drop and the contact angle between the catalyst drop and the crystal play a crucial part in the process of NWs formation. In addition, the contact angle is quite simple to manage technologically by modulating the flow of IV-, III-, or V-substances, altering the temperature growth circumstances, or by using surfactants. However, the questions remain unclear: why, during stationary growth the contact angle  $\beta$  is always greater than 90 ( $\beta > 90$ ) [3, 11, 26, 27] and does not satisfy the condition of the equilibrium contact angle  $\theta$  in Young's equation  $\alpha SL + \alpha L \cos \theta = \alpha S$ , where  $\alpha L$ ,  $\alpha S$ , and  $\alpha SL$  are the specific free energy of the liquid/gas, crystal/gas, and crystal/liquid interfaces [28]. At the same time, for some reason, it is considered a priori that, since the crystallized material is well soluble in the liquid phase of M-catalyst, the drop should wet the crystal surface well. Then, for a catalyst droplet at the vertex of the NW, the validity of Young's equation can be established [28]. It is also unclear how GaAs nanowires self-catalyzed by gallium can grow if the IIIIBV-material is well wetted by liquid-phase Ga drops (Jacobsson et al. [16]), and they must slide down the vertical

side walls of the NWs. In the work of Dubrovskii [11], when modeling the growth of NWs, a controversial statement was formulated that there is no equilibrium contact angle corresponding to the minimum of free surface energy, which includes only a droplet but does not consider the side walls of NWs. In addition, when modeling the growth of NWs, it is erroneously assumed that, under conditions of gravity neutralization, a catalyst droplet can have an energetically preferred nonspherical configuration. In reality, this assumption has no experimental confirmation. In addition, it is still little known how the energy gain occurs during nucleation under the influence of a catalytic liquid at the vertex of NWs [4, 7, 9, 11, 16, 18].

For the regulated development of NWs, a thorough knowledge of the foundations of VLS-growth is essential, and the current confusion surrounding the phenomenon of contact interaction between a catalyst drop and a crystal cannot be tolerated.

In this study, the fundamental aspects of VLS crystallization are examined. We demonstrate that the growth of NWs catalyzed by a liquid droplet is based on a decrease in the activation barrier to crystallization due to the release of excess free energy by the spheroidizing of the droplet in the region of the triple junction of phases, which results in a decrease in the supersaturation required for the growth of the NW's vertex facet at a given rate. During the stationary growth of NWs, the driving force behind the ascent of a droplet is the excess free energy of its outer surface, which leads to the emergence of pressure tending to reduce the free surface. We demonstrate that the increase in free energy associated with an increase in the area of the lateral surface of the crystal in each elementary act of ascent of a droplet upon absorption of a step in a monoatomic layer of height  $h$  is completely negated by a decrease in free energy caused by the disappearance of the step and a decrease in the areas of the outer and inner surfaces of the liquid. Consequently, there exist single values of the angles of inclination of the lateral surface NWs  $d$  and the droplet contact  $b$  at each point of the development of NWs, which correspond to  $FS = \min$  for the growth with a singular end facet and  $FS = 0$  for the growth with a curved end surface. We argue that the wetting hysteresis appears at the vertex of the NWs, the droplet contact angle  $\beta$  does not satisfy the condition for the equilibrium contact angle  $\theta$  in Young's equation, since the conditions of indifferent equilibrium are realized for the drop.

Furthermore, we demonstrate that the contact angle  $b$  is an independent thermodynamic characteristic of the state of a three-phase system, meaning that if it changes, other equilibrium features of the system also change.

## 2. Conditions for the Formation of a Catalyst Droplet

The semiconductor materials crystallizing as NWs in solutions of several catalyst metals, including Au, Pt, Ni, Cu, Ag, Pd, and Ga. In the liquid stage, the pressure is low; therefore, formation during crystallization can only occur with the aid of capillary forces in the absence of external

factors. When gravity is effectively neutralized, capillary forces become apparent. Bond number is characterized by the relative influence of gravitational and capillary forces  $Bo = (\rho_L g L^2 / \alpha_L)$  (where  $L$  is the characteristic size of the liquid meniscus,  $\rho_L$  is the density of the liquid, and  $g$  is the acceleration of gravity) which is a dimensionless quantity [13]. When  $Bo < 1$ , capillarity prevails and when  $Bo > 1$ , gravity prevails. For small bond numbers, the effect of gravity on the catalyst droplet shape can be neglected. If we assume that for the growth of NWs the characteristic linear dimensions of a droplet are in the range of  $10^{-8}/10^{-7}$  m,  $\rho_L \sim 10^3/10^4$  kg/m<sup>3</sup>,  $\alpha_L \sim 1$  J/m<sup>2</sup>, then, the number  $Bo \approx 10^{-4} \ll 1$ . In the absence of external electric fields and substantial temperature gradients, it follows that the nonspherical structure of the catalyst droplet at any value of the contact angle at the NW's vertex may be disregarded. Due to the fact that the impact of gravity may be disregarded, the form of microscopic catalytic droplets in the absence of full wettability of the crystal surface by a liquid is a segment of a sphere. This is true for metal-semiconductor alloys with particle sizes smaller than 105 nm. Therefore, the elongated droplet form anticipated in reference [11] for a Ga-catalyzed GaAs nanowire with transverse dimensions in the range 101–102 nm, when the droplet should slide down the vertical side walls and acquire a nonspherical structure, is practically impossible to achieve.

In the future, while computing the overall change in the free energy of a three-phase system during the development of NWs, we shall no longer account for the component connected with the gravitational impact.

### 3. Growth of NWs with High Wettability of the Crystal Surface ( $\theta < 90^\circ$ )

The formation of NWs is initiated by the production and placement of liquid-phase catalyst droplets on Si, GaAs, InAs, or other substrates. Catalytic particle alloys, such as Me-Si, Me-Ga-As, and Me-In-As, are solutions, not chemical compounds (Me: Au, Pt, Ni, Cu, Ag, Pd, and Ga). In addition to having a low melting point, the aforementioned alloys often have favorable crystal surface wetting characteristics at NWs growth temperatures. Typically, a drop on an extended surface of a growth substrate has a contact angle between 20 and 700 degrees. The droplet form at the vertex of the NWs is a fragment of a sphere with contact angle  $\beta > 90^\circ$ .

**3.1. Growth of Crystals with a Singular Tip Facet.** At tiny, contact angles  $\beta$  of an M-catalyst droplet at the vertex of NWs ( $90^\circ < \beta < 180^\circ$ ), a transverse singular facet (usually {111} for elementary IV-semiconductors,  $(\bar{1}\bar{1}\bar{1})$  B for III-V ZB- and (0001) WZ connections) adjoins the TPL (Figure 1). Crystallization proceeds on the facet by nucleation and the development of monoatomic-height steps [29]. TPL is a closed curve in the shape of a circle encompassing the droplet wetting's perimeter [3, 4].

If the criterion  $\alpha_S - \alpha_L < \alpha_{SL}$  is fulfilled, emission or absorption of TPL growth (nucleation) steps is more

energetically beneath the drop than on the droplet's wetting perimeter [13]. This criterion is satisfied in systems with a soluble solid in a catalytic liquid, for which the values  $\theta < 90^\circ$ , and therefore,  $\alpha_L < \alpha_S$  are characteristics (Figure 2).

Consider a point A on TPL, next to the transverse singular {111} facet. In this scenario, the catalyst droplet will not moisten the NWs' side surfaces of the crystallization front. Crystallization on the {111} face starts by nucleation and growth in the tangential direction in monoatomically tall steps of height  $h$ . The TPL absorb or create the steps so that the forming surface NWs at point A is inclined to the horizontal, i.e., the single facet, i.e., to the singular facet {111}, at the angle  $\delta$  (Figure 3).

The crystal is then elongated by the height of the single-crystal layer  $h$  when the drop is displaced from this distance  $l_S = (h/\sin \delta)$ , {111} facet of the crystallization front is reduced from this distance  $l_{SL} = l_S \cos \delta$ , and the droplet surface is reduced from this distance  $l_L = l_S \cos(\beta - \delta)$ . The change in the free energy associated with a change in the areas of three adjacent surfaces when TPL is displaced from point A to point B will be as follows [30]:

$$F_S = 2\pi r(\alpha_S l_S - \alpha_{SL} l_{SL} - \alpha_L l_L), \quad (1)$$

or per unit TPL length

$$F_S = \frac{h}{\sin \delta} [\alpha_S - \alpha_{SL} \cos \delta - \alpha_L \cos(\beta - \delta)]. \quad (2)$$

In expression (1),  $2\pi r l$  ( $l$  with indexes S, L, and SL) represents the increase in the areas of the crystal/vapor S, liquid/vapor L, and crystal/liquid SL phases, respectively. The sign «-» in front of the second and third terms in equation (2) means that when TPL is displaced from point A to point B, the surface decreases.

For simplicity, in expression (2), we express  $\alpha = (F_S/h)$ . Consequently, the change in the free surface energy of the three-phase system following step absorption (per unit length TPL and per one absorbed step with height  $h$ ) may be expressed as follows:

$$\Delta\alpha = \alpha - \alpha_{SL}. \quad (3)$$

It consists of a term  $-\alpha_{SL}$  (step disappearance) and a term  $\alpha$ -associated with a change in the areas of all three adjacent surfaces [30]. If  $\Delta\alpha < 0$ , then, single-crystal steps can be absorbed (generated) by the separation line of the three phases, forming a lateral surface NWs at the slope angle  $\delta$ . This is possible if  $\varphi_0 < \theta$  (Figure 3). Then, the droplet will move, sliding down the created crystalline layers, reducing the area of its wetting. With such a droplet displacement, the arrangement of three nearby surfaces at TPL alters, leading to increase of the angle  $\varphi_0$  to the equilibrium angle  $\theta$ .

To satisfy the condition  $\Delta\alpha < 0$ , the angle of contraction (expansion) NWs  $\delta$  must correspond to the minimum free energy of the three-phase system after absorption of a monolayer of height  $h$ , i.e., meet the minimum value  $\alpha$ . The minimum value  $\alpha = \alpha_{\min}$  is achieved when, for all possible variations of the shape of the liquid surface (while

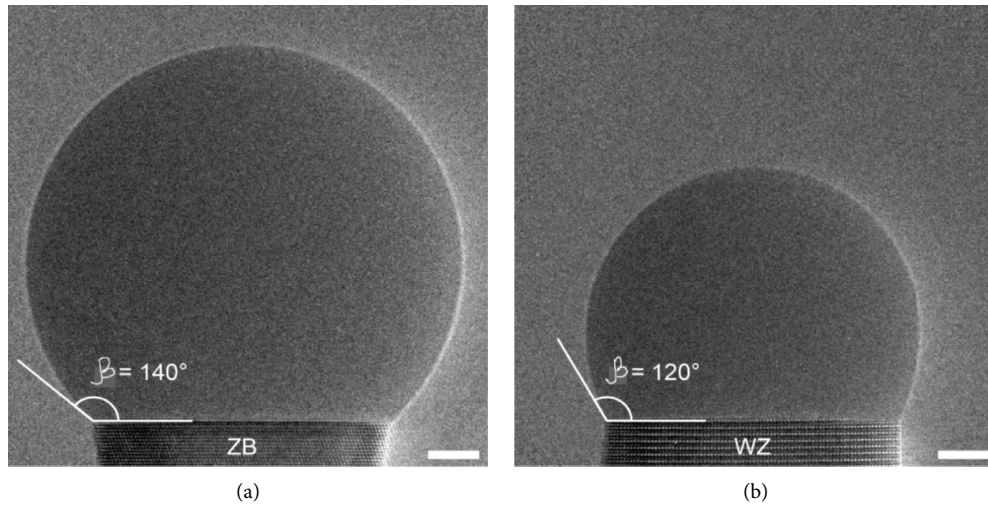


FIGURE 1: Images of vertices of NWs GaAs structures zinblende (ZB) (a) and wurtzite (WZ) (b). Catalyst—Ga [27].

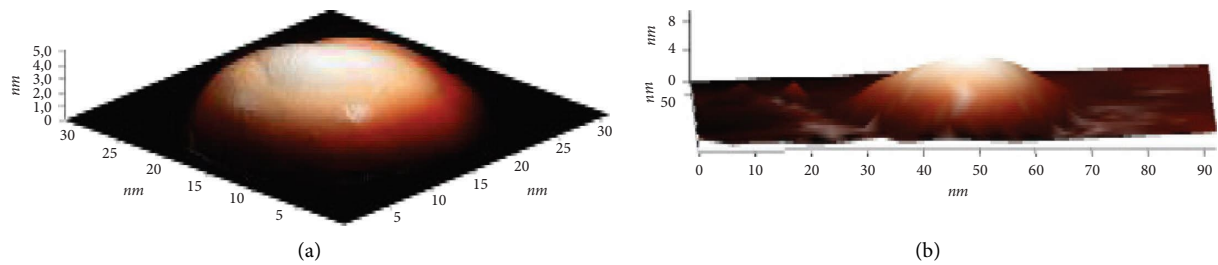


FIGURE 2: SPM images of micro- (a) and nanodroplets (b) of Au-catalyst on the surface of Si-plate with crystallographic orientation {111}.

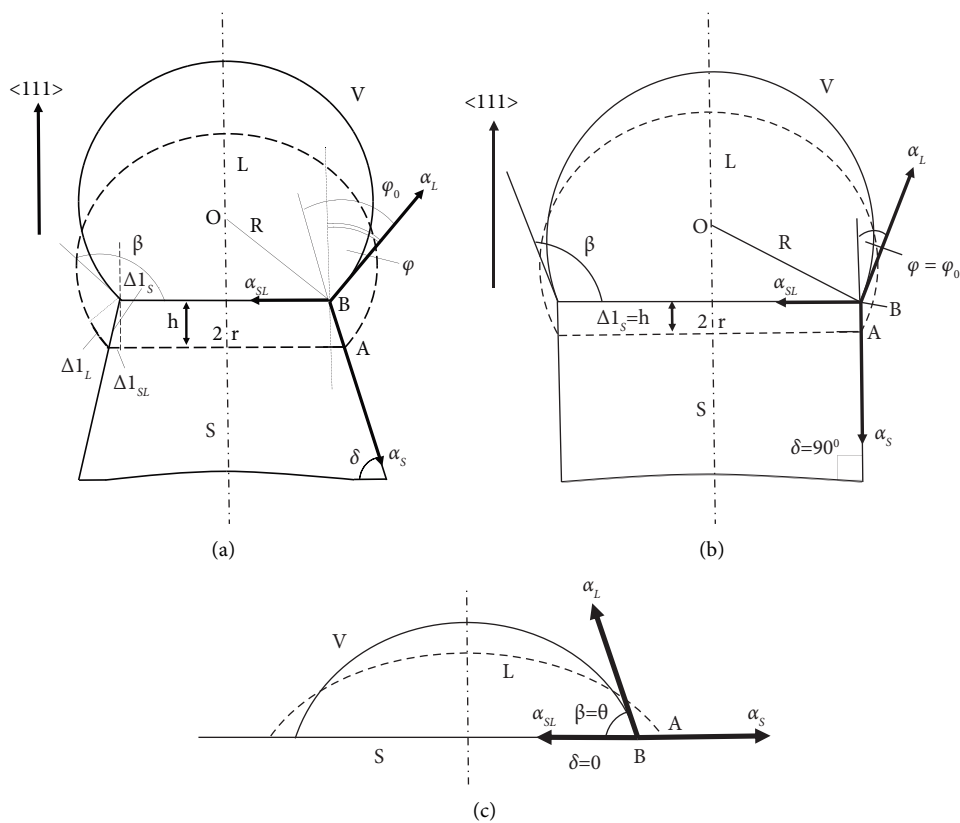


FIGURE 3: Scheme pairing section boundaries of three phases—solid, liquid, and gas for catalyst droplet at vertex tapered ( $0 < \delta < 90^\circ$ ), cylinder ( $\delta = 90^\circ$ ) NWs with transverse facet {111}, and on the substrate ( $\delta = 0$ ).  $\varphi$ —is the angle of the inclination segment surface of the catalyst droplet at the point A on the wetting perimeter to the growth axis NWs and  $\varphi_0$ —is the angle of the inclination segment surface of the droplet to the displacement direction of the TPL.

maintaining its volume), the free energy  $F_S$  remains constant (minimum for stable equilibrium), i.e., at  $(dF_S/d\delta) = 0$ .

Differentiating equation (2) with respect to the slope angle  $\delta$  and equating to zero the derivative, we obtain the condition under which the minimum  $F_S(\delta)$

$$\alpha_L \cos \beta + \alpha_{SL} = \alpha_S \cos \delta. \quad (4)$$

Expression (4) represents the mechanical balance of forces corresponding to the free surface energies of the three phases at the point A on the wetting perimeter. Equation (4) was obtained under the assumption that the anisotropy of the free surface energy of the side  $i$ -facets NWs ( $\sum_i (\partial \alpha_S^i / \partial \delta) = 0$ ), is not considered, the contribution of linear tension is neglected, and the volume of the catalyst droplet  $V$  during the growth of NWs remains constant ( $dV = 0$ ). The latter means that the requirement for the absolute rigidity of the solid and its insolubility in the liquid must be met. The condition for the constancy of the volume of the liquid catalyst droplet and the insolubility of the crystallized material in it can be assumed if we consider the stationary process of growth of NWs at  $T = \text{constant}$  in the absence of chemical entrainment and physical evaporation of the liquid phase material, and neglect the loss of metal due to the dissolution in the solid and surface diffusion.

From expression (4) it follows that at each moment of growth of NWs with a transverse singular facet there are single values of the angles  $\delta$  and  $\beta$ , i.e., such an angle of tapering (expansion) of the crystal  $\delta$  and such a contact angle of the droplet  $\beta$  are realized, which correspond to the minimum increment of the free energy of the three-phase system after absorption of a monolayer of height  $h$ .

$$\delta = \arccos\left(\frac{\alpha_L \cos \beta + \alpha_{SL}}{\alpha_S}\right). \quad (5)$$

Thus, for constant values of the specific free energy of the phase boundaries  $\alpha_S$ ,  $\alpha_L$ , and  $\alpha_{SL}$ , and when the above-mentioned requirements are met, the contact angle  $\delta$  is related by a nonlinear dependence with the contact angle  $\beta$ . The direction of the TPL displacement relative to the droplet surface at point A on the separation line of the three phases adjacent to the transverse singular  $\{111\}$  facet of the crystallization front will be determined by the angle  $\beta - \delta$ , which we will call the growth (crystallization) angle NWs, which, in turn, can be found from the expression (4).

The greater the value of the contact angle  $\beta$  in the range  $0 \leq \beta \leq 180^\circ$ , the larger the angle  $\delta$  will be. At  $\delta = 0$ , in accordance with equations (4) and (5), we obtain the equilibrium condition for a drop lying on a horizontal extended surface as follows:

$$\alpha_L \cos \beta + \alpha_{SL} = \alpha_S. \quad (6)$$

Young's well-known equation is for the mechanical equilibrium of a drop on a flat surface ( $\beta = \theta$ ). TPL displacements here can only be done at an equilibrium angle  $\theta$  horizontally along an extended solid surface.

At  $\delta = 90^\circ$ , equation (4) implies the growth condition for cylindrical NWs of constant diameter [4].

$$\begin{aligned} \alpha_{SL} &= -\alpha_L \cos \beta \\ &= \alpha_L \sin \phi. \end{aligned} \quad (7)$$

Table 1 shows the results of calculation by formula (5) of the slope angle  $\delta$  depending on the value of the contact angle  $\beta$  for the Au-Si system. For the calculation, the following initial values were taken:  $\alpha_L^{\text{Au}} = 0.910 \text{ J/m}^2$ ,  $\alpha_{SL}^{\text{Au-Si}} = 0.455 \text{ J/m}^2$ , and  $\alpha_S^{\text{Si}} = 1,200 \text{ J/m}^2$  [4].

Expressions (3)–(7) give an understanding of why NW narrowing occurs at the initial stage of droplet ascent from the substrate ( $\delta = 0$ ) to reach the cylindrical section ( $\delta = 90^\circ$ ) (Figure 4) [21, 22].

The formation of a cone-shaped initial section NWs is a consequence of ensuring the constancy (zero increment) of the free surface energy of the three-phase system when TPL is displaced during the growth of NWs ( $F_S = \text{const}$ ). The increase in free energy associated with an increase in the area of the lateral surface of the crystal  $2\pi r l$ , in each elementary act of ascent of a liquid droplet upon absorption of a step in a monoatomic layer of height  $h$  is completely compensated by the loss of free energy due to the disappearance of the step and a reduction in the area of the outer and inner surfaces of the liquid droplet. Therefore, to ensure the mechanical equilibrium of the drop on the wetting perimeter (4), the deviation of the angle of inclination of the crystal surface  $\delta$  from zero when the drop rises above the substrate requires a constant increase in the contact angle  $\beta$ . As a result, at  $V = \text{constant}$ , as the drop rises at the initial stage of growth, the wetting perimeter decreases, and a cone-shaped section NWs is formed.

After the drop reaches the stationary growth section, where  $\delta = 90^\circ$ , the balance of forces at the point A, in accordance with equation (6), provides a stable mechanical equilibrium of the catalyst drop and the constancy of the diameter NWs, i.e., the growth of a cylindrical crystal. This form of NWs corresponds to the minimum increment in the surface area of the solid phase for each elementary act of TPL displacement.

However, this does not mean that the appearance of a stepped micromorphology of the lateral facets of the crystal is impossible, since the shape of the drop can deviate from the equilibrium one [20, 31, 32].

Let the lateral dimension of the NWs change. A change in the size of NWs will lead to such a change in the contact angle  $\beta$  that the crystal diameter returns to the unperturbed state. Thus, for example, according to the data presented in Table 1, the stationary value of the contact angle  $\beta$  is  $120^\circ$ , at which  $\delta = 90^\circ$ . With a random decrease in the diameter NWs, the contact angle  $\beta$  becomes greater than  $120^\circ$  ( $\beta > 120^\circ$ ). An increase in  $\beta$  in accordance with equation (4) will require an increase in the angle of inclination of the lateral surface  $\delta$  ( $\delta > 90^\circ$ ). This means that a crystal expanding towards the top should grow. As a result, the crystal diameter returns to its original unperturbed state. Conversely, with a random increase in the diameter, a small decrease in  $\beta$  to  $\beta < 120^\circ$  will lead to a narrowing of NWs ( $\delta < 90^\circ$ ), and consequently, as a result of this, to a decrease in the diameter to a stationary

TABLE 1: Calculated values of the slope angle  $\delta$  depending on the value of the contact angle  $\beta$  for the Au-Si system.

$\beta$ , degree	35, 0	37, 0	42, 3	50, 1	64, 4	80, 80	105, 70	120, 0	125, 0	130, 0	180, 0
$\delta$ , degree	0	10, 0	20, 0	30, 0	45, 0	60, 0	80, 0	90, 0	93, 2	96, 2	117, 0

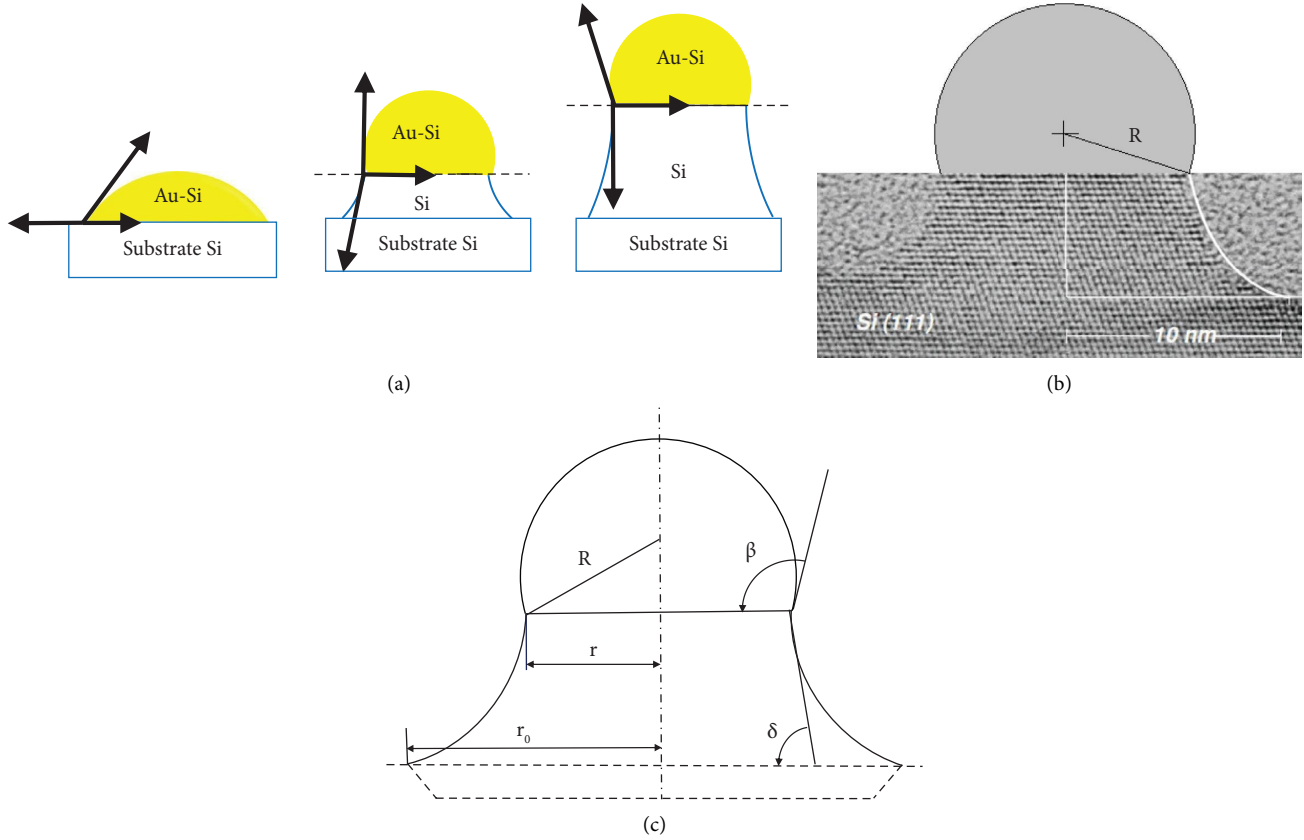


FIGURE 4: The sequence of stages of the formation of NWs pedestals in the Au-Si system in the Au-Si system (a), high-resolution electron microscopic image (JEM-4010) of the initial cone-shaped section of Si NWs epitaxial growth [21] (b), and a schematic representation of NWs at the initial stage of VLS growth (c).

value. Figure 5 is a SEM image illustrating the wavelike profile of the side surface of silicon NWs.

Expression (7) shows that with using NWs, a growth of constant diameter ( $\delta = 90^\circ$ ) in the direction  $\langle 111 \rangle$  for IV semiconductors or  $\langle \bar{1}\bar{1}\bar{1} \rangle$  B ZB and  $\langle 0001 \rangle$  WZ for III-V with isotropy on the wetting perimeter, the contact angle of the catalyst droplet,  $\beta$ , does not consider the free surface energy of the side walls NWs. The steady state contact angle of the droplet in our picture depends on the free surface energies of the solid/liquid and liquid/vapor phase boundaries and does not depend on the free surface energy of the vertical sidewalls of the NW.

Figure 6 shows the calculated plot of the  $\alpha_{\min} = f(\beta)$  dependence for NWs Si, GaAs (ZB), and InAs (ZB) grown with the participation of liquid Au drops. The following quantitative data were used to plot in the graph: (Au-Si)  $\alpha_L^{\text{Au-Si}} = 0.910 \text{ J/m}^2$ ,  $\alpha_{SL}^{\text{Au-Si}} = 0.455 \text{ J/m}^2$ , and  $\alpha_S^{\text{Si}}(111) = 1,200 \text{ J/m}^2$  [4]; (Au-GaAs(ZB))  $\alpha_L^{\text{Au-GaAs}} = 1,000 \text{ J/m}^2$ ,  $\alpha_{SL}^{\text{Au-GaAs}} = 0.600 \text{ J/m}^2$ , and  $\alpha_S^{\text{GaAs}}(\bar{1}\bar{1}\bar{1})B = 1,300 \text{ J/m}^2$  [11]; (Au-InAs(ZB))  $\alpha_L^{\text{Au-InAs}} = 1,000 \text{ J/m}^2$ ,  $\alpha_{SL}^{\text{Au-InAs}} = 0.550 \text{ J/m}^2$ ,

and  $(\bar{1}\bar{1}\bar{1})B = 1,100 \text{ J/m}^2$  [30]. The horizontal dashed lines indicate the free interfacial energy of the crystal/liquid interface for NWs Si, GaAs (ZB), and InAs (ZB).

In the graph Figure 6, on the right and at the top, the region (region II) for NWs Si is marked with a dark background, where the inequality  $\Delta\alpha < 0$  is not satisfied, since to the right and above the intersection points of the curve  $\alpha_{\min} = f(\beta)$  with the horizontal dashed lines  $m_1$ ,  $m_2$ , and  $m_3$ , we have  $\alpha > \alpha_{SL}$ . Points  $m_1$ ,  $m_2$ , and  $m_3$  characterize the maximum possible critical contact angles of catalyst droplets  $\beta = \beta_{\max}$ , at which the growth of NWs with a transverse singular facet is still possible. In other words, the points of intersection of the curves  $\alpha_{\min} = f(\beta)$ . The horizontal dashed lines represent to the contact angles  $\beta$  at which a zero increment of the free energy of the three-phase system is realized ( $\alpha - \alpha_{SL} = 0$ ). At  $\beta > \beta_{\max}$ , the growth of NWs becomes impossible in region II. At very small contact angles  $\beta$ , region III is realized, which is close to complete wetting ( $\theta \rightarrow 0$ ). Figure 6, region III is also highlighted in dark. There is no growth of NWs here either, and the TPL shift can



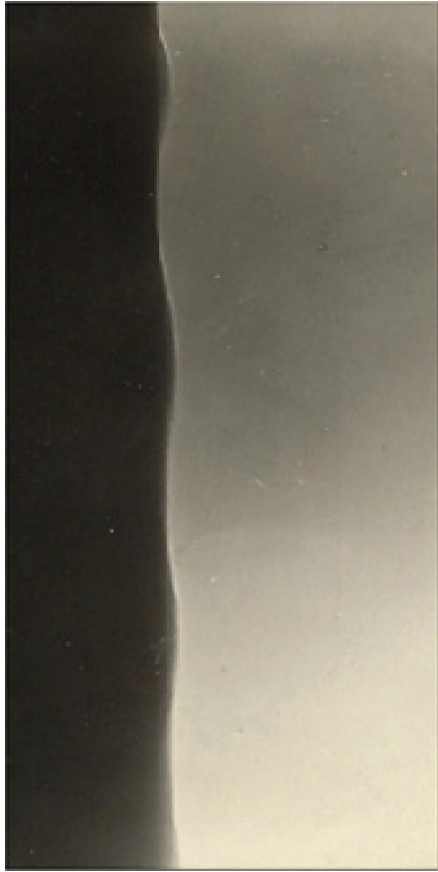


FIGURE 5: The wavelike profile of the side surface of the Si NWs ( $\times 13700$ ).

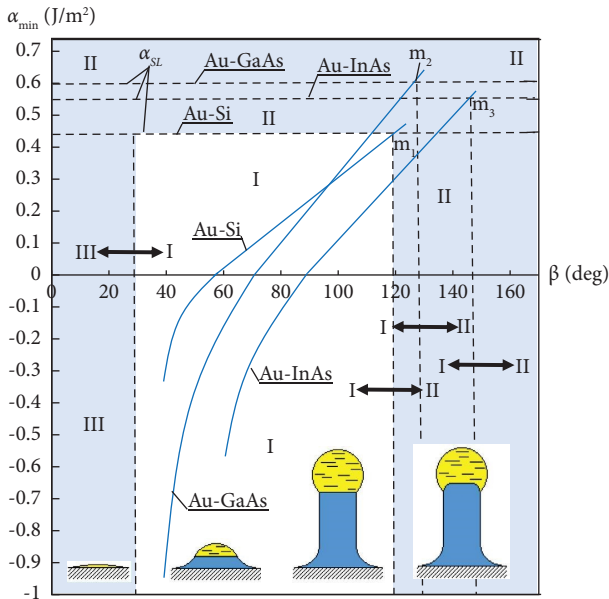


FIGURE 6: Diagram of dependence  $\alpha_{\min}$  on the contact angle  $\beta$  at the NWs vertex in which  $\Delta\alpha < 0$  and the monolayer absorbed (generates) TPL (area I).

be carried out only along the extended surface of the substrate ( $\delta = 0$ ). We see that there is an interval of the contact angles of the catalyst droplet  $\beta$  from  $\beta = \theta > 0$  to  $\beta = \beta_{\max}$ , in which  $\Delta\alpha < 0$  and the monolayers are absorbed (generates) by TPL (region I in Figure 6).

Thus, the graph in Figure 6 shows that the VLS growth of NWs is based on a decrease in the activation barrier to crystallization (region I) due to the release of excess free energy by the spheroidizing drop in the region of the triple junction of phases ( $-(\alpha_{SL} + \alpha_L)$ ) in the process of decreasing its surface area, which results in lowering the supersaturations required for the growth of the NWs vertex facet at a given rate. The driving force for the rise of an M-catalyst droplet during a stationary growth of NWs ( $\delta = 90^\circ$ ) is the excess free energy of its outer surface ( $-\alpha_L$ ), which leads to the appearance of pressure tending to reduce the free surface.

Under steady-state conditions, the radii of the liquid droplet and TPL remain constant during growth [4].

$$\frac{r}{R} = \sqrt{1 - \left(\frac{\alpha_{SL}}{\alpha_L}\right)^2}. \quad (8)$$

Here,  $\Gamma_{де}$ ,  $r$  is the NW radius and  $R$  is the catalyst droplet radius.

Expressions (7) and (8) have a physical meaning if  $\alpha_{SL} < \alpha_L$ , i.e., under the condition of equilibrium wetting of an extended solid surface by a catalyst drop ( $\alpha_{SL} < \alpha_L < \alpha_S$ , therefore,  $\theta < 90^\circ$ ). In addition, it follows from formulas (4) and (7) that the contact angle at the vertex of the cylindrical NWs  $\beta$  is not equal to the contact angle at Young's equilibrium  $\theta$  ( $\beta > \theta$ ). Consequently, the validity of Young's equation cannot be demonstrated [28] for a catalyst droplet on the vertex of cylindrical NWs [28]. In other words, due to the dissolution of the crystallized substance or its separation from the liquid solution of the catalyst droplet at the vertex of NWs, the wetting perimeter of the droplet is not fixed, and it can assume an equilibrium form described by expressions (7) and (8) and does not satisfy the condition of mechanical equilibrium described by the known Young's equation [28].

If the contact angle  $\varphi = \varphi$  for  $\delta = 90^\circ$  is smaller than the equilibrium contact angle  $\theta$ , i.e.,  $\varphi < \theta$ , then, there is a driving force  $FG$  applied to the points on the boundary line of the three phases. Then, the drop will move in the direction of the force  $FG$  until it reaches the state with the contact angle is equal to  $\theta$  [30]. The magnitude of this force per unit length TPL is found from the joint solution of the inequality  $\Delta\alpha < 0$  and equation (6)

$$F_G = \alpha_L (\cos \varphi - \cos \theta) > 0. \quad (9)$$

Inequality (9) is true for  $\varphi < \theta$ . Therefore, the drop will rise to the height of the monoatomic layer  $h$  from the point A if  $\varphi < \theta$ . When  $\varphi = \theta$  is reached, the driving force  $FG$  disappears until the next iteration in the TPL movement. Hence, it follows that the displacement of the droplet with the growth of NWs can be considered process of droplet spheroidization. Expression (9) also shows that the driving

force of the displacement of the catalyst droplet during the growth of NWs is the excess of free energy, the source of which is the outer surface of the droplet. When the drop is displaced to a height  $h$ , its free surface energy decreases. In this case, growth steps are formed along the perimeter of droplet wetting, because of  $\alpha < \alpha_{SL}$ .

To establish the relationship between the contact angles  $\beta$  and  $\theta$ , we jointly solve equations (6) and (7) as follows:

$$\begin{cases} \alpha_{SL} + \alpha_L \cos \beta = 0, \\ \alpha_S - \alpha_L \cos \theta - \alpha_{SL} = 0. \end{cases} \quad (10)$$

As a result, we obtain

$$\frac{\alpha_S}{\alpha_L} = \cos \theta - \cos \beta, \quad (11)$$

or

$$\beta = \arccos \left[ \cos \theta - \frac{\alpha_S}{\alpha_L} \right]. \quad (12)$$

For Si NWs grown through liquid Au-Si droplets and values of free surface energy  $\alpha_L^{Au} = 0.910 \text{ J/m}^2$ , contact angle  $\beta \approx 120^\circ$ , and contact angle  $\theta \approx 30^\circ$  [4], in accordance with equations (10) and (11), we find  $\alpha_{SL}^{Au-Si} = 0.455 \text{ J/m}^2$  and  $\alpha_S^{Si} = 1,366 \text{ J/m}^2$ . For NWs GaAs (ZB), we have  $\alpha_L^{Au} = 1,000 \text{ J/m}^2$ ,  $\beta \approx 125^\circ$ , and  $\theta \approx 20^\circ$  [30], and we have  $\alpha_{SL}^{Au-GaAs} (ZB) = 0.574 \text{ J/m}^2$  and  $\alpha_S^{GaAs} (ZB) = 1,514 \text{ J/m}^2$ .

When growing Si NWs in directions other than  $\langle 111 \rangle$ , such as  $\langle 110 \rangle$ ,  $\langle 100 \rangle$ , or  $\langle 211 \rangle$ , the crystallization front is not a transverse singular facet  $\{111\}$ , and equilibrium at the wetting perimeter is achieved at angles between the front facet crystallization and axis NWs, respectively, equal to  $\sim 125^\circ$ ,  $\sim 145^\circ$  и  $\sim 110^\circ$ .

As a result, for instance, when Si NWs are grown in the direction of 100, the crystal's vertices is a tetrahedral pyramid, and its facets are produced by the 111 [1] plane (Figure 7). The 111 pyramid's facets are angled 550 degrees away from the horizontal.

The equilibrium position of the droplet at the vertex of NWs during stationary growth in the  $\langle 100 \rangle$  direction is similar to the equilibrium position when the pedestal NWs is formed at the point when  $\delta = 25^\circ$ . As you can see, the side walls of crystals grown in the  $\langle 100 \rangle$  direction must contain steps and breaks.

For the realization of the stable growth of NWs with a transverse singular facet ( $\{111\}$ , B or  $\{00\bar{1}\}$ ), it is necessary to ensure a mechanical equilibrium of forces corresponding to the free surface energies of the three phases on the perimeter of droplet wetting. Therefore, to ensure the equilibrium of the drop at the vertex NWs, the contact angle  $\beta$  must satisfy the following conditions:

$$\begin{cases} \alpha_L \cos \beta \leq \alpha_L \cos \theta, \\ \alpha_L \cos(\beta - \delta) \geq \alpha_L \cos \theta. \end{cases} \quad (13)$$

Passing from the cosines, directly, to the angle, we have

$$\begin{cases} \beta \geq \theta, \\ \beta \leq \theta + \delta \text{ При } \delta > 0 \text{ и } \phi \leq \theta \text{ При } \delta = 90^\circ. \end{cases} \quad (14)$$

The first inequality in equations (13) and (14) defines the boundary condition under which a catalyst drop cannot slide along the transverse singular facet, increasing the wetting perimeter and decreasing the contact angle. The second inequality specifies the condition under which the drop cannot descend onto the lateral surface of NWs. Thus, to ensure the equilibrium position of the droplet at the vertex of NWs, the contact angle  $\beta$  should be in the range from  $\theta$  to  $\theta + \delta$  at  $\delta > 0$ . Hence, on a singular extended substrate, when  $\delta = 0$ , the contact angle  $\beta$  is fixed:  $\beta = \theta$  (6). Within the range of variation of the angle specified in inequalities (13) and (14), a drop can maintain an indifferent equilibrium on the wetting perimeter. In actuality, a particular crystal-liquid-vapor combination produces a continuous range of contact angle values. The greatest contact angle of the contact angle hysteresis is known as the advancing contact angle  $\theta_A$ , while the minimum contact angle is known as the receding contact angle  $\theta_R$  ( $\theta_A = \theta + \delta$ ). Using instance, for the data in Table 1,  $\theta = 35^\circ$  and  $\theta_A = 125^\circ$ . Let us explain how the drop wetting hysteresis appears at the NW's vertex.

Let a drop of liquid advancing onto a solid surface, which is the vertex facet of the NW  $\{111\}$ , in the  $x$  direction (Figure 8). Thermodynamic condition spontaneous spreading lies in the fact that the free surface energy  $F_S$  should decrease:  $(dF_S/dx) < 0$ . This corresponds to a continuous decrease in the contact angle of the drop  $\beta$  ( $(d\beta/dx) < 0$ , here  $\beta = f(x)$  is the so-called dynamic contact angle of the drop). For a smooth surface  $\{111\}$  this condition is fulfilled along the entire path. In the presence of a kink at the periphery of the  $\{111\}$  facet, the situation becomes more complicated, since when the liquid flows behind the kink, its surface area increases more strongly than when TPL moves along a smooth surface along the  $x$  direction (dashed line in Figure 8). The surface tension is applied to the new spreading direction AN at an angle  $(\beta - \delta)$ . Using equation (5), the flow condition can be found:  $\beta > (\theta + \delta)$ . At  $\beta < (\theta + \delta)$  a kink at the vertex of the NW represents a barrier that TPL can cross only under external influences (for example, with vibrations) or with sufficiently strong energy fluctuations near TPL. Hence, the contact angle of advancing onto the sidewall surface of the NW  $\theta_A = \theta + \delta$ .

Under conditions when  $\beta > (\theta + \delta)$ , the drop moves onto the sidewalls of the NW. The wetting perimeter, which has descended in this case, makes it possible to grow a crystal expanding towards the top. As a result of the growth of the expanding crystal, the wetting angle of the lateral surface will decrease, and in the limit, reach the receding angle on the lateral facet  $\theta_R = \theta - \delta$ . As a consequence, the TPL must inevitably increase not at the edge of the crystal. At  $\delta = 90^\circ$ , this edge is the line of intersection of the transverse singular facet of the NW with a set of facets of the crystallographic belt with an axis parallel to the axis of the NW.

Thus, the fracture at the NW tip should increase the observed contact angle (during leakage), which is observed in the experiment. The hysteresis of the contact angle or the



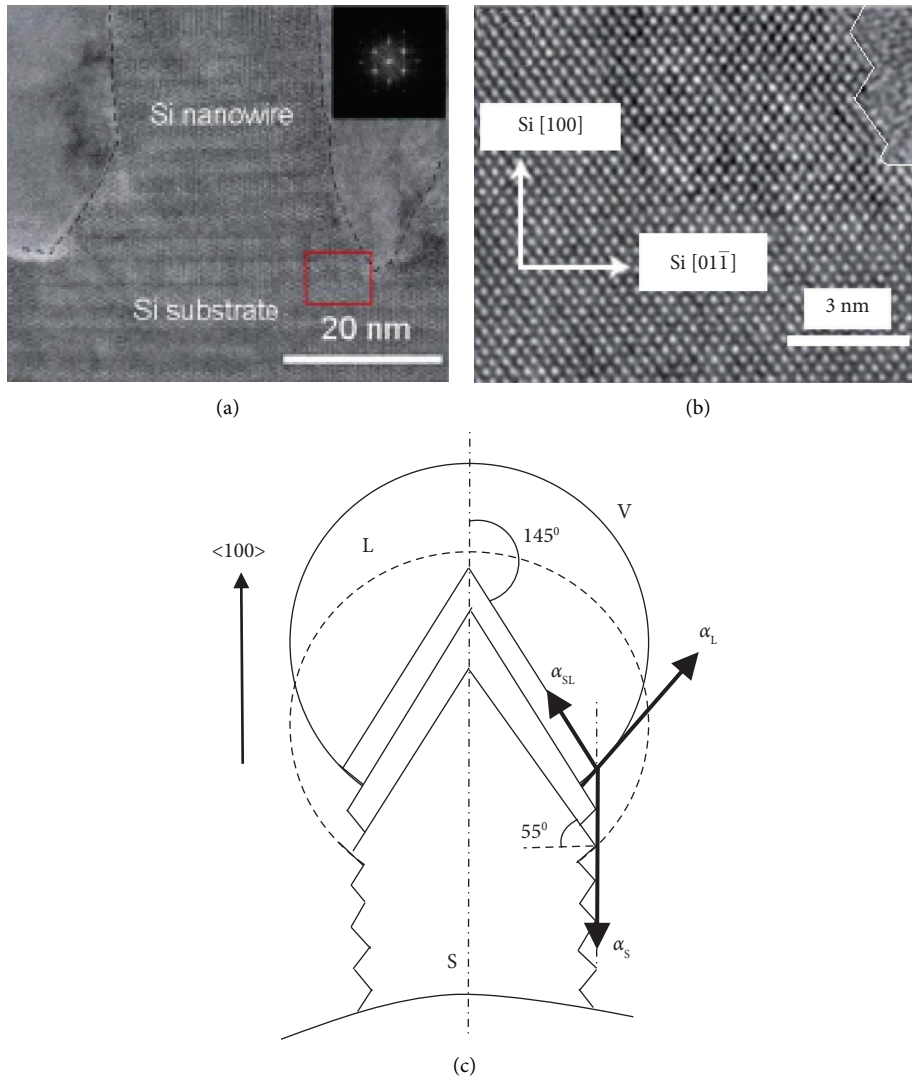


FIGURE 7: TEM image of Si NWs, grown in  $\langle 100 \rangle$  direction on Si substrate (100) (a), enlarged image of a section of this crystal (b) [24], and scheme growing in the  $\langle 100 \rangle$  direction (c).

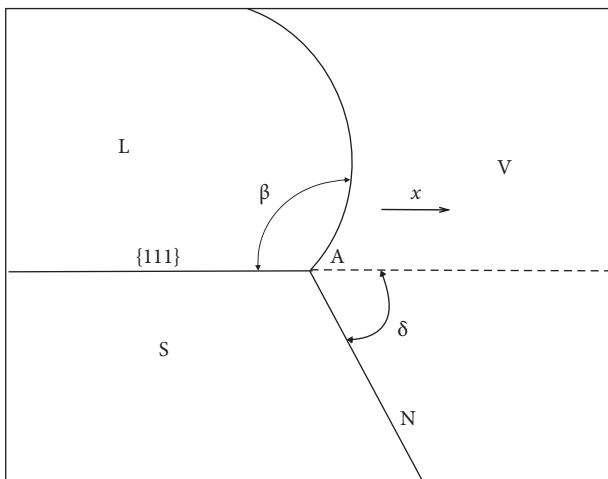


FIGURE 8: Stop of the droplet spreading contour (TPL) at the fracture AN on the NW tip surface.

hysteresis of wettability is appearing at the top of the NW (Figure 9).

It was accepted at  $m = 100\%$ —complete wetting and at  $m = 0$ —complete nonwetting. Leakage angles  $\theta_A$  (curve 1) begin to grow sharply in the triple phase junction area. Therefore,  $\theta_A \rightarrow \theta + \delta$ . Against, the receding contact angles (curve 2) are  $\theta_R \rightarrow \theta$ . The dependence of the contact angles on  $m$  represents a typical hysteresis loop.

During the growth of NWs, the appearance of significant temperature gradients, significant fluctuations in the fluxes of crystallized substances, and concentration disturbances can lead a droplet at the vertex of NWs out of the state of indifferent equilibrium and result in irreversible consequences (splitting a droplet into separate parts and branching NWs, sliding a droplet along a lateral crystal surface, and bending and changes in the spatial direction of NWs [33]).

From expressions (4), (7), and (9) it follows that to achieve stable VLS growth of NWs with a transverse singular

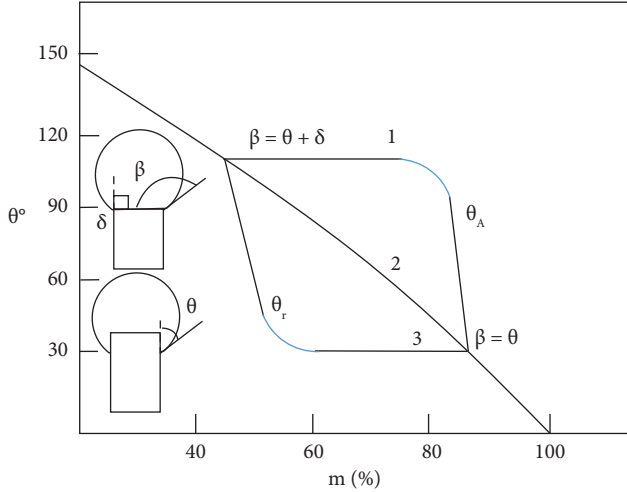


FIGURE 9: Schematic representation of the hysteresis dependence contact angle catalyst droplet on top of the NW for the Me-Si system of the proportion of the degree of wetting  $m$  of well-wetted areas.

facet, metals with a relatively high surface tension  $\alpha_L$  in the liquid state are required as catalysts in comparison with  $\alpha_S$  of the crystal. For Si and Ge, such metals are Au, Pt, Ni, Cu, Ag, Pd, Fe, and Ti [3, 4, 8, 34]. Al, Sn, Zn, Ga, Bi, and In are less favorable [3, 4, 8]. For GaAs, the most suitable metal will be Au [35, 36] and Fe [37], Cu for InP [38], and Pd for InAs [39]. Metals are less suitable for self-catalyzed growth: In for NWs InP and InAs [9] and Ga for GaAs and GaP [3, 9, 40]. For SiC, from the point of view of large  $\alpha_L$ , Fe, Co, Ni, and Pt can be a good catalyst [2]. For thin SiO<sub>2</sub> NWs, due to the contribution of linear tension and curvature of the crystallization front, suitable metals can be Ga, In, and Sn [41, 42].

**3.2. Growth of Nanowires with a Curved Tip Surface.** At very small ( $\beta \rightarrow 90^\circ$ ) or too large ( $90^\circ \ll \beta$ ) contact angles  $\beta$  in the range  $90^\circ < \beta < 180^\circ$  or  $\varphi$  ( $\varphi \rightarrow 0$  or  $0 \ll \varphi$ ) in the range  $0 < \varphi < 90^\circ$ , equation (3) cannot be performed, since the line of separation of the three phases cannot adjoin the transverse singular facet of the crystallization front. Equation (3) is not fulfilled under the conditions for the growth of NWs with a transverse singular facet  $\alpha > \alpha_{SL}$  (regions II and III in Figure 6). Nucleation, in this case, at high supersaturation in the droplet, occurs at the crystal/liquid interface far from the TPL, and the steps cannot be absorbed by the TPL and accumulate in front of it, forming a curved, nonsingular crystallization front with a slope angle  $\psi$  (Figure 10). Here, it is energetically favorable for the catalyst droplet to wet the lateral surface of NWs [17, 27, 29, 43]. As a result, the angle  $\psi$  reaches such a value that the direction of the thermodynamically equilibrium displacement TPL is realized at the angle  $\varphi_0$ , at which  $F_{S(\min)} = 0$  ( $\alpha_{\min} = 0$ ). Here, we also denote by  $\varphi_0$  the angle between the tangent drawn to the meniscus of the liquid phase at the selected triple point A and the direction of the equilibrium displacement of the interface of the three phases.

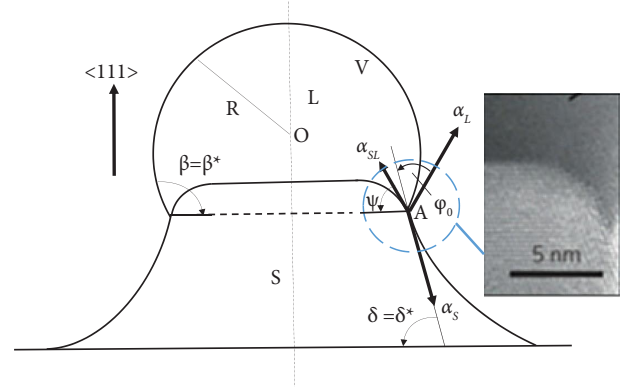


FIGURE 10: Scheme of NW growth at nonsingular end surface. SEM image of the Si NW crystallization front section curved near the TPL.

Thus, under the conditions of a thermodynamically equilibrium displacement of TPL, such angles  $\psi$ ,  $\delta$ , and  $\varphi_0$  are realized at which condition (3) is always fulfilled during the absorption of a monolayer of height  $h$  by TPL, since with an increase in NWs with a curved end surface  $\alpha_{\min} = 0$  and  $\Delta\alpha$  always negative.

Let through closed TPL not pass any close-packed planes. Let us determine the angle of the thermodynamically equilibrium displacement TPL  $\varphi_0$  at the NWs growth. We will not consider the contribution of three-phase boundary linear tension and effect anisotropy of the free surface energy at the crystal/gas and crystal/liquid interfaces. Let us write the components of the force vectors projections, corresponding to the interfaces free surface energy  $\alpha_S$ ,  $\alpha_L$ , and  $\alpha_{SL}$  at point A on TPL to the direction of continuation existing NWs side surface and to the direction perpendicular to it, in the form of an equations' system as follows:

$$\begin{cases} -\alpha_S + \alpha_L \cos \varphi_0 + \alpha_{SL} \sin(90^\circ + \psi - \delta) = 0, \\ -\alpha_L \sin \varphi_0 + \alpha_{SL} \cos(90^\circ + \psi - \delta) = 0. \end{cases} \quad (15)$$

Using the trigonometric identity  $\cos^2 \varphi_0 + \sin^2 \varphi_0 = 1$  and excluding the angle  $(90^\circ + \psi - \delta)$  from the system of equation (15), we express the angle  $\varphi_0$  in an explicit form as follows [44]:

$$\varphi_0 = \arccos\left(\frac{\alpha_S^2 + \alpha_L^2 - \alpha_{SL}^2}{2\alpha_S\alpha_L}\right). \quad (16)$$

According to equation (16), the angle  $\varphi_0$  is a constant value for a given crystallized substance under the given thermodynamic conditions of stationary growth of NWs. The angle  $\varphi_0$  and the TPL shape will determine the shape of the growing NWs with a curved end surface. Therefore,  $\varphi_0$  is the growth angle of crystallizable NWs, similar to the angle  $\beta - \delta$  for the growth of NWs with a singular end facet.

Figure 11 shows the comparative vector diagrams of the forces corresponding to the specific free surface energies of the interfaces of the three phases for the growth of NWs with a nonsingular end surface and with a singular transverse facet. In accordance with the equation of the closed triangle

of forces, the state of stable thermodynamic equilibrium corresponds to only values of the equilibrium angles  $\beta^*$  and  $\delta^*$  (Figure 11(a)). However, in the case of the growth of NWs with a singular facet, due to kinetic restrictions associated with the influence of the anisotropy of the free surface energy of the crystallizable substance, the triangle of forces  $\alpha_S$ ,  $\alpha_L$ , and  $\alpha_{SL}$  is not closed (Figure 11(b)). In this case, the angles  $\beta$  and  $\delta$  cannot reach thermodynamically the equilibrium values  $\beta^*$  and  $\delta^*$ , and for any stationary process, they will correspond to an indifferent equilibrium of droplets on the wetting perimeter, characterized by wetting hysteresis in equations (13) and (14).

Provided that  $\delta = 90^\circ$ , we express the angle  $\psi$  from the second equation of the system of equation (15), and instead of the growth angle  $\varphi_0$ , we substitute its value from equation (16). We get the following equation [17]:

$$\psi = \arccos \left[ \frac{\alpha_L}{\alpha_{SL}} \sqrt{1 - \left( \frac{\alpha_S^2 + \alpha_L^2 - \alpha_{SL}^2}{2\alpha_S\alpha_L} \right)^2} \right]. \quad (17)$$

At  $\psi = 0$ , expression (16) transforms into the condition of mechanical equilibrium of the catalyst droplet of equation (6), which characterizes the growth of NWs of constant diameter when the flat facet of the crystallization front is adjacent to TPL. Surely, in this case  $\varphi = \varphi_0$ .

From the system of equation (14) and expression (16), we obtain the relationship between the angles  $\psi$  and  $\delta$ .

$$\psi = \delta - 90^\circ + \arcsin \left( \frac{\alpha_S^2 + \alpha_{SL}^2 - \alpha_L^2}{2\alpha_S\alpha_{SL}} \right). \quad (18)$$

For the Au-Si system and  $\alpha_L^{Au} = 0.910 \text{ J/m}^2$ ,  $\alpha_S = 1.200 \text{ J/m}^2$ , and  $\alpha_{SL} = 0.450 \text{ J/m}^2$  [4] from equations (15) and (17), we obtain  $\varphi_0 = 19^\circ$  и  $\psi = 49^\circ$ .

To establish the relationship between the growth angle  $\varphi_0$  and the contact angle  $\theta$ , we jointly solve equation (5), where  $\beta = \theta$ , and (16). We get

$$\frac{\alpha_S}{\alpha_L} = \frac{1 - \cos^2 \theta}{2(\cos \varphi_0 - \cos \theta)}. \quad (19)$$

For Si NWs grown by liquid Au-Si droplets and the abovementioned values specific-free surface energy  $\alpha_L^{Au}$ , slope angle  $\beta \approx 120^\circ$  and contact angle  $\theta \approx 30^\circ$  [4], in accordance with equation (18), we find  $\alpha_S^{Si} = 1,366 \text{ J/m}^2$ . For GaAs (ZB) NWs at  $\alpha_L^{Au} = 1,000 \text{ J/m}^2$ ,  $\beta 125^\circ$ , and  $\theta 20^\circ$  [11], we have  $\alpha_S^{Au-GaAs} (ZB) = 0.574 \text{ J/m}^2$  and  $\alpha_{SL}^{GaAs} (ZB) = 1,514 \text{ J/m}^2$ .

#### 4. Growth of NWs with Complete Wettability of the Crystal Surface ( $\theta = 0$ )

With full wetting, when  $\alpha_{SL} + \alpha_L < \alpha_S$ , in accordance with the expression (2) always  $\alpha > \alpha_{SL}$ . This means that, under these conditions, it is energetically more favorable not to form new areas of NWs growth, but rather to shrink the crystal's surface. In this case, on the side walls of the NWs near the TPL, a liquid film of the metal catalyst can form, covering the surface of the crystal. Since the catalyst film is not in

equilibrium, crystallization will occur under it at the interface with NWs. In the absence of a film, under conditions when  $(\beta - \delta) = 0$  and  $\varphi_0 = 0$ , during crystallization, TPL will move along the surface of the drop (Figure 12).

#### 5. Growth of NWs with Poor Wet of the Crystal Surface ( $\theta > 90^\circ$ )

*5.1. Nonwetting ( $90^\circ < \theta < 180^\circ$ ).* Due to the kinetic constraints associated with the energy barrier anisotropic dissolution of the crystallized material in a liquid at given temperatures, the droplet at the vertex does not possess the lowest free surface Gibbs energy in previous instances of wetting a solid phase surface with a catalyst droplet. There is hence no reason to suppose that the droplet's shape at the NW's vertex is thermodynamically stable.

However, in the absence of kinetic constraints due to the dissolution of the required amount of the crystallized substance or its separation from the liquid solution of the catalyst droplet at the crystal/liquid interface, the wetting perimeter of the droplet is not fixed, and the droplet can change the value of the contact angle and assume a thermodynamically stable shape regardless of the increment in wetting perimeter. In this instance, the assumption of a catalyst droplet with a constant volume will not be met ( $dV \neq 0$ ). However, after reaching thermodynamic equilibrium, the shape droplet will satisfy the condition  $\sum \alpha_{IJ} S_{IJ} = \min$  и  $\sum \alpha_{IJ} dS_{IJ} = 0$  (where  $\alpha_{IJ}$  and  $dS_{IJ}$ —specific free surface energy and the increment in the area of individual parts of area  $I$  in contact with the phases  $J$  at  $V = \text{const}$ ).

Let us write the first condition of thermodynamic equilibrium catalyst droplet on vertex cylindrical NW [43].

$$F_S^{\text{drop}} = [2\alpha_L (1 + \sin \phi) + \alpha_{SL} \cos^2 \phi] \pi R^2 = \min, \quad (20)$$

where the first term is the free surface energy of the liquid/vapor interface and the second is the interphase energy of the crystal/liquid interface.

We differentiate with the angle  $\phi$  and equate the derivative (20) to zero. Let us obtain an expression that describes the thermodynamic equilibrium shape of a droplet, corresponding to the minimum value of free surface energy:

$$-\alpha_{SL} \sin \phi + \alpha_L = \alpha_{SL} \cos \beta + \alpha_L = 0. \quad (21)$$

To satisfy condition (21), it should be  $\alpha_{SL} > \alpha_L$ . This is possible, example, for a droplet saturated with a crystallizable substance, which nonwet the horizontal substrate, as shown in Figure 13 ( $\theta > 90^\circ$  and  $\alpha_{SL} > \alpha_S > \alpha_L$ ).

If  $\alpha_{SL} > \alpha_S$ , then, the full compensation increment free energy of the crystal surface by TPL absorption of by a single crystal layer of thickness  $h$  will be at any contact angle  $\beta$  (or  $\phi$ ) of a catalyst droplet, since always  $\alpha < \alpha_{SL}$  and inequality (3) satisfied. Therefore, when equation (20) is satisfied, due to the independence of the shape droplet from  $\alpha_S$ , NWs can grow with a constant diameter direct from the substrate

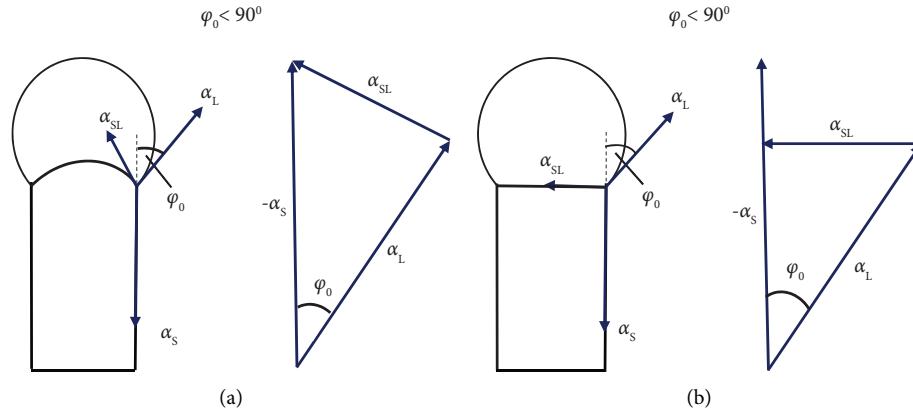


FIGURE 11: Vector diagram of forces corresponding to the specific free energies of the three-phase interfaces for the NWs growth with a nonsingular end surface (a) and a singular transverse facet (b).

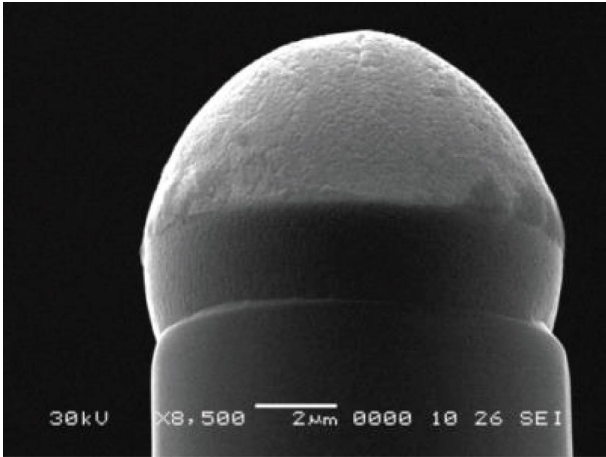


FIGURE 12: SEM image of the vertex of Si NWs, at the TPL displacement on the catalyst droplet surface during the formation of a recrystallization layer.

(Figure 14(a), 14(b), and 14(d)), i.e., without the initial cone shape (Figure 14(c)).

Full thermodynamic equilibrium of droplets (20) can be maintained by dissolving or separating the crystallized substance [23, 24] and by constantly feeding the M-catalyst material during the NWs growth [24]. In the first case, it was found that Si dissolution in liquid droplet metal catalysts ( $M = \text{Au, Ni, Pt, and Cu}$ ) has been shown to impair the wettability of the Si surface by these metals, sharply increasing the contact angle: from  $25^\circ$ – $55^\circ$  for pure metals to  $105^\circ$ – $130^\circ$  for M–Si under near-equilibrium conditions [43]. Moreover, the NWs grow without forming a tapered pedestal at the base. For Si NWs grown through liquid droplets Au–Si and values of free surface energy  $\alpha_L^{\text{Au}} = 0.910 \text{ J/m}^2$  and contact angle  $\varphi = 30^\circ$  ( $\beta = 120^\circ$ ) [4] in according with equation (15) found  $\alpha_{SL}^{\text{Au-Si}} = 1.82 \text{ J/m}^2$ . For NWs in Figure 1, for GaAs(ZB), we have  $\alpha_L^{\text{Ga}} = 0.711 \text{ J/m}^2$  [11] and  $\varphi = 50^\circ$  ( $\beta = 140^\circ$ ). Then  $\alpha_{SL}^{\text{Ga-GaAs}} = 0.928 \text{ J/m}^2$ . For GaAs(WZ)  $\varphi = 30^\circ$  ( $\beta = 120^\circ$ ), we obtain  $\alpha_{SL}^{\text{Ga-GaAs}} = 1,422 \text{ J/m}^2$ .

5.2. *Absence Wetting* ( $\theta = 180^\circ$ ). In the complete absence of crystal surface wetting ( $\alpha_S + \alpha_L < \alpha_{SL}$ ,  $\beta = 180^\circ$  and  $\varphi = 90^\circ$ ), i.e., in the absence of atomic adhesion between the crystal and the liquid phase, a gas layer separates the catalyst drop from the crystal support. In this instance, it can be assumed that the gas phase completely “wets” the existing liquid phase on the solid surface. Therefore, in the absence of a droplet wetting the crystal surface, simply a phase transition happens at the interface with vapor, and NWs do not grow. Therefore, the liquid forms spherical droplets on the solid surface (Figure 15), but the contact angle  $\beta = 180^\circ$  is not observed in nature.

## 6. Contact Angle of Catalyst Droplet

The previous equation shows that the contact angle  $\beta$  (or  $\varphi$ ), whose sine (or cosine for  $\varphi$ ) at  $\delta = 90^\circ$  (see equation (7)) characterizes the ratio of the disperse of the catalyst droplet  $D_R = 1/R$  and the crystal  $D_r = 1/r$ , that is, the ratio of the surface area per unit volume of the droplet and the crystal. Therefore, it follows that the contact angle serves as an independent thermodynamic characteristic of the system’s state, whose variation influences other equilibrium features of the system.

This is demonstrated by the following example, which characterizes the effect of the contact angle on the parameters of a three-phase system.  $\alpha_S < \alpha_{SL} + \alpha_L$  and  $V = \text{constant}$ . If a catalyst drop is on the vertex of cylindrical NWs, and the contact angle  $\beta > 90^\circ$ , then, the crystal/liquid interface will be small and the amount of crystallized substance adsorbed on it from the supersaturated drop will also be small. If the drop is located on an extended wetted substrate, then  $\beta = \theta < 90^\circ$ , and the liquid phase spreads over the surface of the solid, increasing the wetting area. Then, the total amount of crystallized substance adsorbed at the crystal/liquid interface will increase, and its concentration in the volume of the liquid phase will decrease. All this will happen with a constant volume of liquid, temperature, pressure, number of components, and phases. The equilibrium in the system will change only due to a change in the value of the contact angle

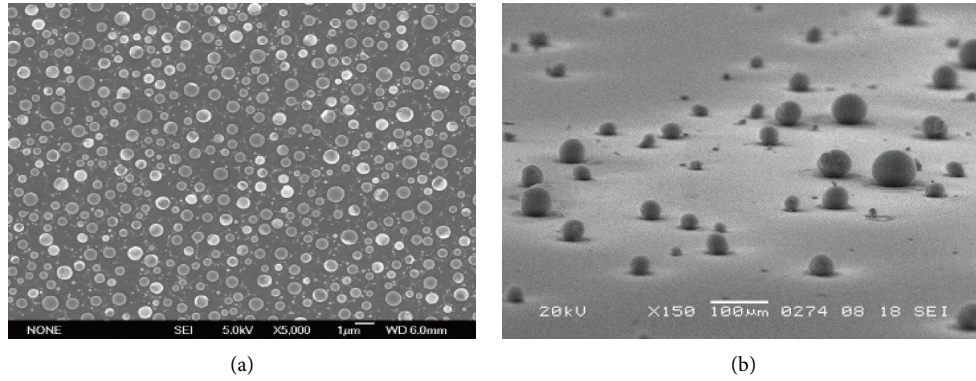


FIGURE 13: SEM image of liquid-phase Sn-droplets on a silicon wafer [45] (a) and (b), the nonwet substrate ( $\theta > 90^\circ$ ).

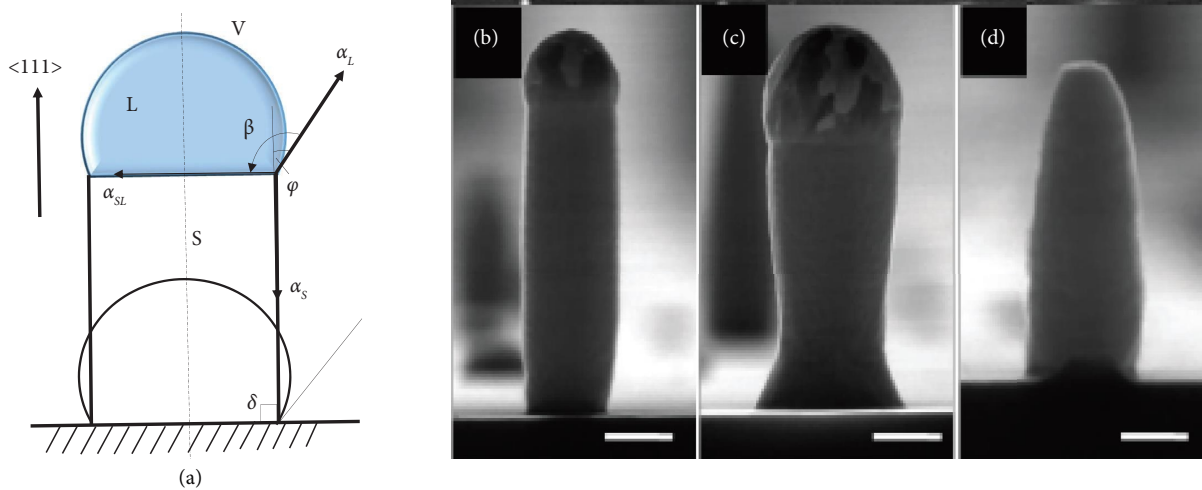


FIGURE 14: Scheme of NW growth without the formation of a cone-shaped base (a) and SEM images of Si NWs grown on a Si (111) substrate with an Au catalyst and different morphologies [24] (b) without a cone-shaped base with a constant diameter, (c) with a cone-shaped pedestal at the base and a diameter increasing towards the apex, and (d) with a straight base and a diameter decreasing in height. Droplets (b) and (d) continuously received additional Au, which compensated for the narrowing of the stem at the base. Scale 100 nm.

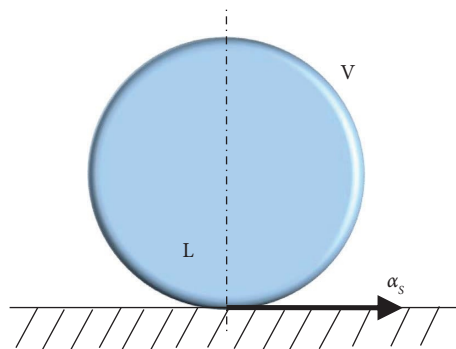


FIGURE 15: Liquid on the solid surface at  $\beta = 180^\circ$  forms spherical drops.

$\beta$  (the ratio of the specific surfaces of the crystal/liquid and liquid/vapor interfaces).

If we neglect the presence of phase boundaries, under the conditions considered, the number of degrees ( $C = K - P$ ) is equal to unity (the number of components  $K = 2$  (for example, Si and Au), the number of phases  $P = 1$  (melt),

temperature  $T = \text{constant}$  and pressure  $p = \text{constant}$ ). This means that only the concentration of the crystallizable substance in the droplet can be arbitrarily changed, the other parameters will take on the corresponding values. With a constant amount of crystallizable substance in the drop, the state of the system is invariant, which corresponds to



a degree of freedom equal to zero ( $C = 0$ ). However, when the contact angle  $\beta$  changes, the distribution of the crystallizable substance in the system changes. This means that the system under consideration has an additional free degree. Thus, the contact angle  $\beta = \arcsin(D_R/D_r)$  acts as an intense feature of the system, similar to the concentration of the crystallizable component.

Therefore, it can be seriously considered as a full-fledged thermodynamic parameter of the system. The influence of the contact angle on the course of crystallization processes of NW growth considered in this article is an additional substantiation of this conclusion. On the basis of these findings, we will now examine some crucial aspects of the NW growth.

## 7. VLS Mechanism

VLS is the only known instance of crystallization involving the simultaneous involvement of more than two phases. A further distinguishing characteristic of VLS crystallization is the occurrence of a triple phase boundary, which is absent from conventional crystal formation techniques. Consequently, the growth mechanism of NWs is complex and poorly understood. Other growth methods, such as vapor-solid-solid, also exist (VSS). Nevertheless, regardless of whether crystal development proceeds by the VLS or VSS mechanism, both mechanisms depend on the catalyst material at the top of the NWs for growth. However, now we can answer two crucial questions: (i) what is the physical nature of the VLS growth mechanism, and (ii) where do the gas-phase epitaxy of elementary semiconductor films through a liquid metal layer “stop” and the VLS growth of NWs “begin?” The physical nature of the mechanism of the VLS growth of NWs in semiconductors lies in the effective reduction of the activation barrier for the nucleation of monoatomic layers (steps) on the TPL as a result of the melt atoms compensating for most of the free energy expanded on the formation of unsaturated bonds in the growing crystal (3). In situations in which a drop in the amount of Me-catalyst to micro- and nanoscales results in the formation of capillary stability (Figure 5), we are dealing with VLS growth of NWs. When capillary stability is absent, epitaxial films form.

## 8. Catalyst Selection

In addition to the conditions under which the catalyst for the growth of NWs must form a liquid phase with the material being grown at the crystallization temperature, it must also have a low saturated vapor pressure, not form refractory compounds with the crystallized substance, and have a low distribution coefficient within the crystal so as not to contaminate the crystal with foreign impurities. Taking into mind the preceding notions, the needs for Me-catalysts must be increased for the stable growth of NWs. The catalyst at the top of the NW should have the optimal liquid phase drop contact angle (see Section 2). When a metal drop well wets the surface of the growth substrate at the growth temperature (for example, Ag or Al on the Si surface at

$T = 773\text{--}1273\text{ K}$ ) or when there is almost no wetting, one should not anticipate steady growth of NWs (Zn, In, Sn, or Pb on the Si surface at the same temperatures). According to the aforementioned requirement, in addition to the metals known from the literature [46], metals such as Os, Ir, Ru, Rh, Sc, and Cd can be used to create silicon NWs.

As applied to compounds, the preceding criteria significantly restrict the selection of catalysts. It is challenging to select a solvent capable of providing the same and sufficient high solubility for all components of the molecule. There is one instance in which the intricate character of the join appears to make the decision simpler. Self-catalyzed development of NWs occurs when a component of the crystalline molecule itself acts as a catalyst [47, 48].

## 9. Self-Catalyzed Growth

The employment of a component of a crystalline compound as a catalyst for the formation of NWs of III–V compounds gives some advantages. Analyze them using the formation of GaAs NWs in the Ga–GaAs system as an example [47, 49].

First, the use of foreign metals as catalysts for the formation of NWs, which inevitably results in the crystal's contamination with foreign impurities, is prohibited. Second, the solubility of Ga in GaAs crystals is exceedingly low, allowing for the growth of extremely pure crystals. By manipulating the Ga and As fluxes in the reaction zone, it is feasible to regulate the phase switching of the resultant NWs: zinc blende (ZB) and wurtzite (WZ).

However, such catalysts have inherent disadvantages that limit their use for growing NWs by the VLS mechanism:

- The metal component (Ga, In, and Tl) has, as a rule, a sufficiently high saturated vapor pressure and is gradually consumed due to transport into the gas phase, as a result of which it is necessary to continuously feed the crystallization zone with this material;
- The very high sensitivity of the droplet size of the catalyst, as Ga to the V/III flux ratio when an unbalanced As/Ga ratio is used;
- Possible polymorphic transformations in the vicinity of the ZB  $\leftrightarrow$  WZ phase transition temperature and the formation of unstable high-temperature NW modifications.

In addition to the abovementioned list of disadvantages, based on the results of our analysis, it is necessary to single out one more disadvantage characteristic of catalysts for the self-catalyzed growth of NWs. A drop of a solution of the metal component of an A<sup>III</sup>B<sup>V</sup> semiconductor compound usually wets the crystal surface well, which, as was said in Section 3.1, should hinder the self-catalyzed growth of NWs.

## 10. The Motion of the Catalyst Drop Substance

The aforementioned models assume that the volume of the catalyst droplet remains constant during the growth of NWs ( $V = \text{const}$ ). On thin crystals, however, the migration of Au atoms from small catalyst droplets to larger ones has been



seen, both on the substrate's flat surface and from the top of one crystal to the top of an adjacent crystal [50]. Au atoms quickly migrate over the Si surface from small droplets to larger ones, and this process (the so-called Ostwald maturation) occurs in 2-3 minutes. The force causing migration is the size gradient between adjacent droplets. This migration results in a change in the volume of the drop ( $dV \neq 0$ ). Consider this process in detail.

Let the volume flow of catalyst drop substances  $a_v$  (volume of substance carried away from a unit of surface per unit of time) be constant and the shape of the drop is not changing during the growth of NW. It can then be written as follows:

$$2\pi R a_v dt = -2\pi R dR, \quad (22)$$

where  $t$  is the duration of the process and  $R$  is the radius of the drop. Integrating the left and right parts of expression (22), it will be found that

$$t = -a_v^{-1} R + C, \quad (23)$$

where  $C$  is the integration constant. The integration constant is determined from condition  $R = R_0$  at time  $t = 0$ . Taking into account the latter, an expression for changing the NW radius over time can be written as follows:

$$t = a_v^{-1} (R_0 - R), \quad (24)$$

where  $R_0$  is the initial radius of the drop. An equation relating NW length  $l$  and change of its radius ( $R_0 - R$ ) is obtained by multiplying the left and right parts of equation (24) by the NW growth rate  $v$  and considering it to be a constant ( $v = v_0$ ):

$$l = v_0 a_v^{-1} (R_0 - R). \quad (25)$$

It follows from expression (25) that the NW radius should decrease linearly at  $a_v = \text{constant}$  as NW grows. As a result, conical-shaped pointed crystals are formed.

Thus, despite the fact that Hannon [50] demonstrated in 2006 that the hypothesis and the shape of the catalyst droplet does not change during growth by the VLS mechanism is false, expression (25) demonstrates that all the NW growth models we have developed for various wetting conditions are applicable (via  $R_0$ ) in the case of substance loss by the catalyst droplet ( $R_0 - R$ ).

## 11. The NW Growth in Case of Unintentional Introduction of Contaminants

As demonstrated in Section 3.1, the physical nature of the nucleation mechanism of growth of NWs of semiconductors as a result of the combined vapor-liquid-droplet-crystal phase transition consists of an effective decrease in the activation barrier for the nucleation of monoatomic layers at the three-phase contact line as a result of the release of excess free surface energy by the spheroidizing drop on top of the growing crystal. The surplus free surface energy is the driving force behind droplet motion and NW development. In addition to catalytic particles spheroidizing during

growth, other sources of this excess free energy include the outer surface of background impurities unintentionally introduced into the reaction zone due to the insufficient purity of the materials used, the inner surface of pores in porous materials or the outer surface of protrusions of rough substrates, defects in the crystal lattice of microcrystallites, fine and imperfect grains of this phase with high angular momentum, and defects in the crystal lattice. All of the listed and related sources delivered indiscriminately into the reaction area for the formation of NWs are, in reality, growth process contaminants. For instance, [51] demonstrated that the preparation of silicon wafers with potassium hydroxide results in the unintended formation of many NWs due to the presence of Fe contaminating particles. It is also known that native NWs can grow on porous substrates, in human kidneys, plant cells, etc. Therefore, it is essential to closely control the purity of the materials utilized and the sterility of the growth process when cultivating NWs.

## 12. The Bimetals-Based Catalysts

Let us analyze the growth of Si NWs with bimetallic catalysts and the effect of the vapor→solid→solid (VSS) mechanism using the example of Cu-Sn-Si [52] from the standpoint developed by us. The phase diagram of Sn-Si is of the eutectic type, in which the eutectic point is strongly shifted towards Sn. This means low solubility of Si in liquid Sn at Si NW growth temperatures of 773–873 K. The Cu-Si phase diagram reveals the presence of a number of intermetallic compounds that are stable at a temperature of  $T < 1,135$  K. Surface tension of pure copper is significantly greater than that of molten silicon ( $1.280 \text{ J/m}^2$  for Cu against  $0.800 \text{ J/m}^2$  for Si). This indicates that the dissolving of Si in a drop of liquid Cu should reduce the solution's specific free surface energy. Therefore, silicon should localize near surface Cu atoms and produce an intermetallic compound in the Cu-Sn bimetallic catalyst (copper silicide  $\text{Cu}_3\text{Si}$  [52]). The creation of a solid phase in a liquid-phase solution of Cu-Sn-Si means that the steps created on the TPL in a liquid solution enriched in Sn at the boundary with the solid silicide phase Sn-Cu<sub>3</sub>Si cannot be absorbed (inequality  $\Delta\alpha < 0$  (3) is not satisfied) and will instead collect in front of it. In this instance, Si atoms can rearrange themselves into a twin configuration [30, 52]. The energy of the twin boundary and the accumulation of unabsorbed steps in front of the boundary inhibit the creation of the very first twin nucleus. Nonetheless, if a twin nucleus has formed, fast development of the twin occurs (because to the lower energy), displacing the regular crystal on the {111} Si facet.

## 13. Conclusions and Outlooks

It is shown that the VLS growth of NWs is based on a decrease in the activation barrier to crystallization due to the release of excess free energy by a spheroidizing droplet catalyst in the region of the triple junction of phases, and a decrease in the supersaturations is necessary for the growth of the singular vertex facet of NWs at a given rate. The closed interface of three phases at the vertex of NWs is a permanent

source of steps at the periphery of the crystallization front under the drop, which creates conditions for continuous growth, which is qualitatively similar to the step of a screw dislocation on the crystal surface in the mechanism of layered spiral growth, but energetically more favorable than a spiral.

The driving force of the displacement of the catalyst droplet in the process of stationary VLS growth of NWs FG at  $\varphi < \theta$  is the excess of free energy, the source of which is the outer surface of the droplet  $F_G = \alpha_L (\cos \phi - \cos \theta) > 0$ . In each elementary act of movement of a catalyst droplet upon absorption of a step of a monoatomic layer with a height  $h$ , the increment of free energy associated with an increase in the area of the lateral surface of the crystal is completely compensated by a decrease in free energy due to the disappearance of the step and a reduction in the area of the outer and inner surfaces of the liquid phase  $\Delta\alpha < 0$ . The angles of inclination of the lateral surface NWs  $\delta$  and the slope angle  $\beta$  of a drop are realized that correspond to the minimum free energy associated with a change in the areas of three adjacent surfaces adjacent to the TPL after the absorption of a growth step with a singular facet, i.e.,  $FS = \min$  and  $FS = 0$  for growing NWs with a curved end surface. This condition is fulfilled at a mechanical equilibrium of forces corresponding to the specific free energy of the interfaces of the three phases, at the wetting perimeter of the droplet:  $\alpha_{SL} = -\alpha_L \cos \beta = \alpha_L \sin \phi$  at  $\delta = 90^\circ$ . However, it is necessary to consider the influence of the wetting hysteresis: on the vertex singular facet NWs, the catalyst droplet will assume an equilibrium shape if the contact angle  $\beta$  is in the range of angles from  $\theta$  to  $\theta A = \theta + \delta$ , which does not satisfy the contact angle  $\theta$  condition in Young's equation, because the conditions of indifferent equilibrium are realized.

The growth (crystallization) angle, that is, the angle that determines the direction of TPL displacement relative to the droplet surface, is found by the following conditions: for the growth of NWs with a singular end facet:  $\phi_0^\infty = \beta - \delta$ , where  $\delta = \arccos(\alpha_L \cos \beta + \alpha_{SL}/\alpha_S)$ ; for the growth of NWs with a curved end facet adjoin TPL  $\phi_0 = \arccos(\alpha_S^2 + \alpha_L^2 - \alpha_{SL}^2/2\alpha_S\alpha_L)$ .

It is shown that the contact angle of a catalyst droplet at the vertex of NWs  $\beta = \arcsin(D_R/D_r)$  can be considered as an independent and full-fledged thermodynamic parameter of a three-phase system.

The fundamental aspects of VLS crystallization outlined in this article should be useful both for a deeper understanding of the mechanism of one-dimensional growth of NWs as a whole, and for its individual sides and individual growth systems for obtaining elementary IV semiconductors, III-V and II-VI compounds, and oxide materials. Wetting phenomena have been studied for almost 200 years. However, some fundamental problems have not yet been resolved. The contact angle hysteresis almost always accompanies wetting. The development of wetting control methods based on the use of the regularities of the hysteresis of the contact angle of the catalyst drop at the top of the NW in the future will undoubtedly make it possible to stabilize the parameters of the vapor-liquid-crystal crystallization

process in the absence of rigid shaping and to obtain NWs with reproducible geometric and electrophysical characteristics.

## Data Availability

Any data and information used to support the findings of this study will be provided by the corresponding author upon request.

## Conflicts of Interest

The authors declare that there are no conflicts of interest regarding the publication of this article.

## Acknowledgments

This study was carried out with the financial support of the Russian Foundation for Basic Research No. 22-22-00449, <https://rscf.ru/project/22-22-00449/%C2%BB> on the equipment of the Central Public Institution "Nano-electronics and Nanotechnological Devices" of Voronezh State Technical University. The authors would like to thank Editage (<http://www.editage.com>) for English language editing.

## References

- [1] R. S. Wagner and W. C. Ellis, "Vapor-liquid-solid mechanism of single crystal growth," *Applied Physics Letters*, vol. 4, no. 5, pp. 89-90, 1964.
- [2] G. A. Bootsma, W. F. Knippenberg, and G. Verspui, "Growth of SiC whiskers in the system SiO<sub>2</sub>-CH<sub>2</sub> nucleated by iron," *Journal of Crystal Growth*, vol. 11, no. 3, pp. 297-309, 1971.
- [3] E. I. Givargizov, "Fundamental aspects of VLS growth," *Journal of Crystal Growth*, vol. 31, pp. 20-30, 1975.
- [4] V. A. Nebol'sin and A. A. Shchetinin, "Role of surface energy in the vapor-liquid-solid growth of silicon," *Inorganic Materials*, vol. 39, no. 9, pp. 899-903, 2003.
- [5] L. Samuelson, "Self-forming nanoscale devices," *Materials Today*, vol. 6, no. 10, pp. 22-31, 2003.
- [6] Y. Wang, V. Schmidt, S. Senz, and U. Gosele, "Epitaxial growth of silicon nanowires using an aluminium catalyst," *Nature Nanotechnology*, vol. 1, no. 3, pp. 186-189, 2006.
- [7] F. Glas, J. C. Harmand, and G. Patriarche, "Why does wurtzite form in nanowires of III-V ZB semiconductors?" *Physical Review Letters*, vol. 99, no. 14, Article ID 146101, 146106 pages, 2007.
- [8] V. Schmidt, J. V. Wittemann, and U. Gosele, "Growth, thermodynamics, and electrical properties of silicon nanowires," *Chemical Reviews*, vol. 110, no. 1, pp. 361-388, 2010.
- [9] V. G. Dubrovskii, *Nucleation Theory and Growth of Nanostructures*, Springer, Berlin, Germany, 2014.
- [10] J.-C. Harmand, G. Patriarche, F. Glas et al., "Atomic step flow on a nanofacet," *Physical Review Letters*, vol. 121, no. 16, Article ID 166101, 166109 pages, 2018.
- [11] V. G. Dubrovskii, "Development of growth theory for vapor-liquid-solid nanowires: contact angle, truncated facets, and crystal phase," *Crystal Growth & Design*, vol. 17, no. 5, pp. 2544-2548, 2017.
- [12] F. Panciera, Z. Baraissov, G. Patriarche et al., "Phase selection in self-catalyzed GaAs nanowires," *Nano Letters*, vol. 20, no. 3, pp. 1669-1675, 2020.

- [13] V. A. Nebol'sin, D. B. Suyatin, A. I. Dunaev, and A. F. Tatarenkov, "Capillary stability of vapor-liquid-solid crystallization processes and their comparison to Czochralski and Stepanov growth methods," *Journal of Crystal Growth*, vol. 463, pp. 46–53, 2017.
- [14] A. Zang, G. Zheng, and C. M. Lieber, *Nanowires: Building Blocks for Nanoscience and Nanotechnology*, Springer, Berlin, Germany, 2016.
- [15] C.-Y. Wen, J. Tersoff, K. Hillerich et al., "Periodically changing morphology of the growth interface in Si, Ge, and GaP nanowires," *Physical Review Letters*, vol. 107, no. 2, Article ID 25503, 2011.
- [16] D. Jacobsson, F. Panciera, J. Tersoff et al., "Interface dynamics and crystal phase switching in GaAs nanowires," *Nature*, vol. 531, pp. 317–322, 2016.
- [17] V. A. Nebol'sin, N. Swaiikat, and A. Vorob'ev, "Development of growth theory for vapor-liquid-solid nanowires: wetting scenario, front curvature, growth angle, linear tension, and radial instability," *Journal of Nanotechnology*, vol. 2020, Article ID 5251823, 9 pages, 2020.
- [18] J. Tersoff, "Stable self-catalyzed growth of III-V nanowires," *Nano Letters*, vol. 15, no. 10, pp. 6609–6613, 2015.
- [19] A. D. Gamalski, C. Ducati, and S. Hofmann, "Cyclic supersaturation and triple phase boundary dynamics in germanium nanowire growth," *Journal of Physical Chemistry C*, vol. 115, no. 11, pp. 4413–4417, 2011.
- [20] V. A. Nebol'sin, A. A. Shchetinin, A. N. Korneeva et al., "Development of lateral faces during vapor-liquid-solid growth of silicon whiskers," *Inorganic Materials*, vol. 42, no. 4, pp. 339–345, 2006.
- [21] V. Schmidt, S. Senz, and U. Gösele, "The shape of epitaxially grown silicon nanowires and the influence of line tension," *Applied Physics A*, vol. 80, no. 3, pp. 445–450, 2005.
- [22] V. A. Nebol'sin, A. I. Dunaev, E. V. Zotova, and M. A. Zavalishin, "Epitaxial growth of silicon whiskers without tapering at the base," *Inorganic Materials*, vol. 46, no. 10, pp. 1039–1044, 2010.
- [23] V. A. Nebol'sin, A. I. Dunaev, M. A. Zavalishin, G. A. Sladkich, and A. F. Tatarenkov, "About a fundamental uncertainty of the contact angle of the catalyst drop on the top of the nanowire," *Journal of Applied Physics*, vol. 129, no. 16, 2012.
- [24] Z. Zang, *Epitaxial Semiconductor Nanostructure Growth with Templates (PhD Tesis)*, Martin-Luther-Universität Halle-Wittenberg, Halle, Germany, 2010.
- [25] K. A. Dick, P. Caroff, J. Bolinsson et al., "Control of III-V nanowire crystal structure by growth parameter tuning," *Semiconductor Science and Technology*, vol. 25, no. 2, Article ID 24009, 2010.
- [26] M. S. Song and Y. Kim, "Growth of Bimodal Sn-Catalyzed CdS Nanowires by Using Tin Sulfide," *Journal of Physical Chemistry C*, vol. 118, no. 11, pp. 5988–5995, 2014.
- [27] G. A. Bootsma, W. F. Knippenberg, and G. Verspui, "Phase transformations, habit changes and crystal growth in SiC," *Journal of Crystal Growth*, vol. 8, no. 4, pp. 341–353, 1971.
- [28] T. Young, "An essay on the cohesion of fluids," *Philosophical Transactions of the Royal Society of London*, vol. 95, pp. 65–87, 1805.
- [29] M. Tornberg, C. B. Maliakkal, D. Jacobsson, K. A. Dick, and J. Johansson, "Limits of III-V nanowire growth based on droplet dynamics," *Journal of Physical Chemistry Letters*, vol. 11, no. 8, pp. 2949–2954, 2020.
- [30] V. A. Nebol'sin, A. I. Dunaev, A. F. Tatarenkov, and S. S. Shmakova, "Scenarios of stable Vapor→Liquid Droplet→Solid nanowire growth," *Journal of Crystal Growth*, vol. 450, pp. 207–214, 2016.
- [31] F. M. Ross, J. Tersoff, and M. C. Reuter, "Sawtooth faceting in silicon nanowires," *Physical Review Letters*, vol. 95, no. 14, Article ID 146104, 2005.
- [32] J. Bolinsson, P. Caroff, B. Mand, and K. A. Dick, "Wurtzite-zincblende superlattices in InAs nanowires using a supply interruption method," *Nanotechnology*, vol. 22, Article ID 509901, 2011.
- [33] V. A. Nebol'sin, A. I. Dunaev, A. A. Dolgachev et al., "Critical parameters of the vapor-liquid-solid growth of silicon whiskers," *Inorganic Materials*, vol. 47, no. 1, pp. 11–15, 2011.
- [34] S. Kodambaka, J. Tersoff, M. C. Reuter, and F. M. Ross, "Germanium nanowire growth below the eutectic temperature," *Science*, vol. 316, no. 5825, pp. 729–732, 2007.
- [35] F. Glas, "Chemical potentials for Au-assisted vapor-liquid-solid growth of III-V nanowires," *Journal of Applied Physics*, vol. 108, no. 7, Article ID 73506, 2010.
- [36] K. A. Dick, "A review of nanowire growth promoted by alloys and non-alloying elements with emphasis on Au-assisted III-V nanowires," *Progress in Crystal Growth and Characterization of Materials*, vol. 54, no. 3-4, pp. 138–173, 2008.
- [37] I. Regolin, V. Khorenko, W. Prost et al., "GaAs whiskers grown by metal-organic vapor-phase epitaxy using Fe nanoparticles," *Journal of Applied Physics*, vol. 101, no. 5, Article ID 54318, 2007.
- [38] K. Hillerich, M. E. Messing, L. Reine Wallenberg, K. Deppert, and K. A. Dick, "Epitaxial InP nanowire growth from Cu seed particles," *Journal of Crystal Growth*, vol. 315, no. 1, pp. 134–137, 2011.
- [39] H. Xu, Y. Wang, Y. Guo et al., "Defect-free <110> zinc-blende structured InAs nanowires catalyzed by palladium," *Nano Letters*, vol. 12, no. 11, pp. 5744–5749, 2012.
- [40] M. Premila et al., "Mechanism of self-assembled growth of ordered GaAs nanowire rrays by metalorganic vapor phase epitaxy on GaAs vicinal substrates," *Nanotechnology*, vol. 23, no. 2, Article ID 25601, 2012.
- [41] Z. W. Pan, Z. R. Dai, C. Ma, and Z. L. Wang, "Molten gallium as a catalyst for the large-scale growth of highly aligned silica nanowires," *Journal of the American Chemical Society*, vol. 124, pp. 1817–1822, 2002.
- [42] J. Zhang, Y. Yang, S. Ding, J. Li, and X. Wang, "Bimetal Ga-Sn catalyzed growth for the novel morphologies of silicon oxide nanowires," *Materials Science and Engineering: B*, vol. 150, no. 3, pp. 180–186, 2008.
- [43] V. A. Nebol'sin, A. Vorob'ev, and N. Swaiikat, "A new understanding of the vapor-liquid-solid mechanism of nanowire growth," *Inorganic Materials*, vol. 56, no. 4, pp. 346–352, 2020.
- [44] A. Valery, "Nebol'sin, vladimir A. Yuriev, nada swaiikat, valeria V. Korneeva on the stability of catalyst drops at the vapor-liquid-SolidContact during the nanowires," *Growth/NANOSYSTEMS*, vol. 14, no. 4, pp. 381–392, 2022.
- [45] A. Zamchiy, E. Baranov, and S. Khmel, "New approach to the growth of SiO<sub>2</sub> nanowires using Sn catalyst on Si substrate," *Physica Status Solidi C*, vol. 11, no. 9, pp. 1397–1400, 2014.
- [46] P. C. McIntyre and A. Fontcuberta i Morral, "Semiconductor nanowires: to grow or not to grow?" *Materials Today Nano*, vol. 9, Article ID 100058, 2020.
- [47] S. Ambrosini, M. Fanetti, V. Grillo, A. Franciosi, and S. Rubini, "Vapor-Liquid-Solid and vapor-solid growth of self-catalyzed GaAs nanowires," *AIP Advances*, vol. 1, no. 4, Article ID 42142, 2011.

- [48] D. S. Dhungana, N. Mallet, P.-F. Fazzini, G. Larrieu, F. Cristiano, and S. R. Plissard, "Self-catalyzed InAs nanowires grown on Si: the key role of kinetics on their morphology," *Nanotechnology*, vol. 33, no. 48, Article ID 485601, 2022.
- [49] V. G. Dubrovskii, T. Xu, A. D. Álvarez et al., "Self-equilibration of the diameter of Ga-catalyzed GaAs nanowires," *Nano Letters*, vol. 15, no. 8, pp. 5580–5584, 2015.
- [50] J. B. Hannon, S. Kodambaka, F. M. Ross, and R. M. Tromp, "The Influence Of The Surface Migration Of Gold On The Growth Of Silicon Nanowires," *Nature*, vol. 440, pp. 69–71, 2006.
- [51] A. D. Dashtestani, A. Moeinian, J. Biskupek, and S. Strehle, "Contamination-Assisted rather than metal catalyst-free bottom-up growth of silicon nanowires," *Advanced Materials Interfaces*, vol. 8, no. 22, Article ID 2101121, 2021.
- [52] E. Ngo, W. Wang, P. Bulkin et al., "Liquid-Assisted vapor-solid-solid silicon nanowire growth mechanism revealed by *in situ* TEM when using Cu-Sn bimetallic catalysts," *Journal of Physical Chemistry C*, vol. 125, no. 36, Article ID 19773, 19779 pages, 2021